



REALIZATION OF PHOTONIC CRYSTAL BASED DIGITAL DEVICES



PROJECT REPORT

Submitted by

ABISHEKA PRIYAN T R

AKASH B

ARAVIND L

DINESH M

in partial fulfillment for the award of the degree

of

BACHELOR OF ENGINEERING

in

**ELECTRONICS AND COMMUNICATION
ENGINEERING**

K. RAMAKRISHNAN COLLEGE OF TECHNOLOGY

(An Autonomous Institution, Affiliated to Anna University Chennai and Approved by AICTE, New Delhi)

**SAMAYAPURAM – 621 112
MAY, 2025**



REALIZATION OF PHOTONIC CRYSTAL BASED DIGITAL DEVICES



PROJECT REPORT

Submitted by

ABISHEKA PRIYAN T R

AKASH B

ARAVIND L

DINESH M

*in partial fulfillment for the award of the degree
of*

BACHELOR OF ENGINEERING

in

ELECTRONICS AND COMMUNICATION ENGINEERING

K. RAMAKRISHNAN COLLEGE OF TECHNOLOGY

(An Autonomous Institution, Affiliated to Anna University Chennai and Approved by AICTE, New Delhi)

SAMAYAPURAM – 621 112

MAY, 2025

K. RAMAKRISHNAN COLLEGE OF TECHNOLOGY
(AUTONOMOUS)

SAMAYAPURAM– 621 112

BONAFIDE CERTIFICATE

Certified that this project report titled “**REALIZATION OF PHOTONIC CRYSTAL BASED DIGITAL DEVICES** ” is the bonafide work of **ABISHEKA PRIYAN TR (811721106005), AKASH B (811721106006), ARAVIND L (811721106012), DINESH M (811721106032)** who carried out the project under my supervision. Certified further, that to the best of my knowledge the work reported herein does not form part of any other project report or dissertation on the basis of which a degree or award was conferred on an earlier occasion on this or any other candidate.

SIGNATURE

Dr.S.SYEDAKBAR, M.E.,Ph.D.,

HEAD OF THE DEPARTMENT

Assistant Professor

Department of Electronics and
Communication Engineering

K Ramakrishnan College of Technology
(Autonomous)

Samayapuram – 621 112

SIGNATURE

Ms.S.GEERTHANA, M.E.,(Ph.D)

SUPERVISOR

Assistant Professor

Department of Electronics and
Communication Engineering

K Ramakrishnan College of Technology
(Autonomous)

Samayapuram – 621 112

Submitted for the viva-voce examination held on

INTERNAL EXAMINER

EXTERNAL EXAMINER

DECLARATION

We jointly declare that the project report on “**REALIZATION OF PHOTONIC CRYSTAL BASED DIGITAL DEVICES**” is the result of original work done by us and to best of our knowledge, similar work has not been submitted to “**ANNA UNIVERSITY CHENNAI**” for the requirement of Degree of **BACHELOR OF ENGINEERING**. This project report is submitted on the partial fulfillment of the requirement of the award of Degree of **BACHELOR OF ENGINEERING**.

Signature

ABISHEKA PRIYAN T R

AKASH B

ARAVIND L

DINESH M

Place: Samayapuram

Date:

ACKNOWLEDGEMENT

It is with great pride that we express our gratitude and in-debt to our institution “**K. Ramakrishnan College of Technology (Autonomous)**”, for providing us with the opportunity to do this project.

We are glad to credit the honorable and admirable chairman **Dr.K.RAMAKRISHNAN, B.E.**, for having provided the facilities during the course of our study in college.

We would like to express our sincere thanks to our beloved Executive Director **Dr.S.KUPPUSAMY, MBA, Ph.D.**, for forwarding our project and offering adequate duration in completing our project.

We would like to thank **Dr.N.VASUDEVAN, M.Tech., Ph.D.**, Principal, who gave opportunity to frame the project with full satisfaction.

We whole heartedly thank **Dr S. SYEDAKBAR, M.E., Ph.D.**, Head of the Department, Department of Electronics and Communication Engineering for providing his encouragement in pursuing this project.

We express our deep and sincere gratitude to our project guide, **Ms. S. GEERTHANA M.E.,(Ph.D.)**, Assistant Professor, Department of Electronics and Communication Engineering, for her incalculable suggestions, creativity, assistance and patience which motivated us to carry out this project.

We render my sincere thanks to Course Coordinator **Dr.G. REVATHI M.E., Ph.D.**, Assistant Professor, and other staff members for providing valuable information during the course.

We wish to express our special thanks to the officials and Lab Technicians of our departments who rendered their help during the period of the work progress.

ABSTRACT

Photonic crystals have emerged as a promising technology in developing digital devices due to their ability to control and manipulate light at the nanoscale. By employing periodic dielectric structures, photonic crystals create bandgaps that prevent certain wavelengths of light from propagating, allowing for precise control of light flow. This unique property allows for designing highly efficient, compact, and low-power photonic devices that operate faster than traditional electronic devices. This study explores the realisation of digital devices using photonic crystal technology, focusing on the design and simulation of components such as photonic crystal waveguides, resonators, and switches. We present designs that utilise photonic bandgap effects to achieve efficient data transmission and processing. Through simulations, the proposed devices demonstrate enhanced performance in terms of speed, scalability, and integration potential with existing photonic and electronic systems. The findings indicate that photonic crystals can enable new functionalities in digital devices, such as all-optical processing and high-speed data transfer, making them a viable solution for future photonic integrated circuits (PICs). This research contributes to advancing photonic-based digital device technologies, potentially impacting fields from telecommunications to quantum computing.

TABLE OF CONTENTS

CHAPTER	TITLE	PAGE NO
	ABSTRACT	V
	LIST OF FIGURES	IX
	LIST OF TABLES	X
	LIST OF ABBREVIATIONS	XI
1	INTRODUCTION	1
	1.1 INTRODUCTION	1
	1.1.1 Overview of Photonic Crystals	1
	1.1.2 Importance of Optical Communication and Digital Technologies	2
	1.1.3 Purpose and Scope of the Report	3
	1.2 FUNDAMENTALS OF PHOTONIC	3
	1.2.1 Definition and Basic Principles	4
	1.2.2. Comparison with Electronic Band Structures	5
	1.2.3 Types of Photonic Crystals	6
	1.2.3.1 One-Dimensional (1D) Photonic Crystals	6
	1.2.3.2 Two-Dimensional (2D) Photonic Crystals	6

	1.2.3.3 Three-dimensional (3D) Photonic Crystals	7
	1.2.3.4 Photonic Bandgaps (PBGs) and Their Significance	8
	1.3. FABRICATION TECHNIQUES FOR PHOTONIC CRYSTALS	8
	1.3.1 Lithographic methods (e-beam lithography, nanoimprint lithography)	9
	1.3.1.1 Electron Beam Lithography (e-beam Lithography)	9
	1.3.1.2 Nanoimprint Lithography (NIL)	10
	1.3.2 Advanced Nanofabrication Methods (3D printing, laser interference lithography)	10
	1.3.2.1 3D Printing for Nanofabrication	11
	1.3.1.2 Laser Interference Lithography (LIL)	11
	1.3.3 Self-Assembly Techniques for Photonic Crystal Fabrication	12
	1.3.3.1 Colloidal Crystallization	12
	1.3.3.2 Block Copolymer Templating	13
2	LITERATURE SURVEY	15
3	EXISTING METHOD AND PROPOSED METHOD	24
	3.1 INTRODUCTION	24
	3.2 DEFINITION	24

3.3	RING RESONATOR	25
3.3.1	Square and quasi-square-shape PCRR	25
3.3.2	Dual curved-shape PCRR	26
3.3.3	Hexagonal-shape PCRR	27
3.3.4	45-deg-square shape PCRR	28
3.3.5	Diamond-shape PCRR	29
3.3.6	X-shape PCRR	30
3.4	STRUCTURE OF PHOTONIC CRYSTAL RING RESONATOR (PHCRR)	31
3.5	WORKING PRINCIPLE OF PHOTONIC CRYSTAL RING RESONATOR (PHCRR)	33
4	PROPOSED METHOD	36
4.1	STRUCTURE DESIGN	36
4.2	OPERATING PRINCIPLE	38
4.2.1	Working Principle of Add Drop Filter	40
4.3	HEXAGONAL DUAL-RING RESONATOR	41
4.3.1	Working Principle of Dropping Wavelength Filter	42
4.4	HEXAGONAL DUAL-RING RESONATOR	44
4.4.1	Operating Principle	45
4.4.2	Working Principle	46

	4.5 COMPARISON OF THE PROPOSED METHODS	48
	4.6 POWER LEVEL CALCULATION	49
5	SOFTWARE REQUIREMENTS	51
	5.1 INTRODUCTION	51
	5.2 OPTI FDTD SOFTWARE	51
	5.3 DESIGNING STEPS TO CREATE	52
	5.4 APPLICATIONS	58
	5.5 SOURCES	59
	5.6 MATERIALS	59
	5.7 SIMULATOR	59
6	RESULT AND DISCUSSION	60
	6.1 SIMULATION RESULTS	60
	6.2 DISCUSSION	62
7	CONCLUSION	65
	7.1 CONCLUSION	66
	7.2 FUTURE ENHANCEMENT	67
	REFERENCES	68

LIST OF FIGURES

FIGURE NO	TITLE	PAGE NO
1.1	One-dimensional (1D) Photonic Crystals	6
1.2	Two-dimensional (2D) Photonic Crystals	7
1.3	Three-dimensional (3D) Photonic Crystals	7
3.1	Square and quasi-square-shape PCRR	26
3.2	Dual curved-shape PCRR	27
3.3	Hexagonal-shape PCRR	28
3.4	45-deg-square shape PCRR	29
3.5	Diamond-shape PCRR	30
3.6	X-shape PCRR	31
3.7	Structure of Photonic Crystal Ring Resonator (PhCRR)	33
3.8	Wavelength of 1.57um	34
3.9	Wavelength of 1.53um	34
4.1	Schematic of the basic ring resonator structure with an input port and 3 output ports.	37
4.2	Add Drop Filter	39
4.3	Hexagonal Dual-Ring Resonator	42
4.4	Hexagonal Dual-Ring Resonator	46
5.1	Design PBG Crystal Structure	53
5.2	Silicon Rod Dimension Settings	54
5.3	Silicon Rod Dimension View	55

5.4	Silicon Cell Off Settings	56
5.5	Observation Point	57
6.1	Output for Add Drop Filter	60
6.2	Output Hexagon Dual Ring Resonator	61
6.3	Output Hexagon Dual Ring Resonator	61
6.4	Dropping Wavelength Filter	62

LIST OF TABLES

TABLE NO	TITLE	PAGE NO
4.1	Simulation Parameters	38
4.2	Comparison of the Proposed Methods	39
4.3	Power Level Calculation	49

LIST OF ABBREVIATION

ADC	- ANALOG-TO-DIGITAL CONVERTER
CMOS	- COMPLEMENTARY METAL-OXIDE- SEMICONDUCTOR
CSK	- COLOR-SHIFT KEYING
FDTD	- FINITE-DIFFERENCE TIME DOMAIN
IoT	- INTERNET OF THINGS
LCoS	- LIQUID CRYSTAL ON SILICON
LED	- LIGHT EMITTING DIODE
MAN	- METROPOLITAN-AREA NETWORKS
OCC	- OPTICAL CAMERA COMMUNICATION
PML	- PERFECTLY MATCHED LAYERS
SOI	- SILICON-ON-INSULATOR
UPML	- UNIAXIAL PERFECTLY MATCHED LAYER
WDM	- WAVELENGTH DIVISION MULTIPLEXING

CHAPTER 1

INTRODUCTION

1.1 INTRODUCTION

1.1.1 Overview of Photonic Crystals

Photonic crystals are engineered optical materials with a periodic structure that influences light propagation, similar to how atomic lattices control electron movement in solids. Their defining characteristic is the photonic bandgap (PBG), which restricts certain wavelengths of light from travelling through the structure. This property enables precise control over light transmission, making photonic crystals a crucial technology in optical communication, signal processing, and digital computing. The ability to manipulate light at the nanoscale has led to numerous innovations in modern optical systems. Photonic crystals can be classified into one-dimensional (1D), two-dimensional (2D), and three-dimensional (3D) structures based on their periodicity. 1D photonic crystals are commonly used in optical filters and reflectors, whereas 2D and 3D photonic crystals enable more complex light control, essential for applications such as waveguides, resonators, and advanced optical circuits.

One of the most significant applications of photonic crystals is in optical communication networks. Traditional electronic components face limitations such as signal degradation, heat dissipation, and energy inefficiency. In contrast, photonic crystal-based components, such as low-loss waveguides and optical filters, improve data transmission efficiency and reduce energy consumption in fibre-optic communication. Beyond communication, photonic crystals are paving the way for next-generation computing, including optical and quantum computing. Photonic crystal-based logic gates, optical transistors, and high-speed interconnects offer promising alternatives to traditional semiconductor electronics, enhancing computing performance while minimizing power consumption. With ongoing research and technological advancements, photonic crystals are expected to play a pivotal role in high-speed data processing, energy-efficient computing, and next-generation optical communication systems, shaping the future of modern digital technologies.

1.1.2 Importance of Optical Communication and Digital Technologies

The rapid growth of global data traffic has created an increasing demand for high-speed, energy-efficient, and reliable communication systems. Traditional electronic circuits and copper-based networks face limitations such as signal degradation, latency, and power inefficiency. Optical communication, which uses light for data transmission, has emerged as a superior alternative, offering higher bandwidth, lower latency, and minimal signal loss over long distances. Photonic crystals play a crucial role in enhancing optical communication by enabling precise control over light propagation. Their ability to create photonic bandgaps (PBGs) allows for the design of low-loss waveguides, optical filters, and resonators, essential for modern fiber-optic communication systems. These components significantly improve data transmission speeds, reduce signal interference, and enhance energy efficiency, making them vital for telecommunications and high-speed networking.

Beyond communication, photonic crystals are transforming digital technologies, particularly in optical computing and data processing. Unlike traditional semiconductor-based electronics, optical computing harnesses the speed of light to perform operations at unprecedented speeds. Photonic crystal-based components such as optical switches, logic gates, and transistors provide faster and more scalable alternatives to electronic circuits, reducing power consumption and heat generation.

Photonic crystals are being integrated into emerging technologies such as artificial intelligence (AI), quantum computing, and biomedical sensing. Their ability to manipulate light at the nanoscale enables applications in high-speed data centres, optical interconnects, and advanced imaging systems. As the demand for faster and more efficient data transmission continues to grow, photonic crystals provide a promising pathway toward overcoming the limitations of traditional electronics. With ongoing research and advancements, they are expected to play a pivotal role in shaping the future of next-generation optical communication and digital computing technologies.

1.1.3 Purpose and Scope of the Report

The purpose of this report is to provide a comprehensive analysis of photonic crystals and their significant role in advancing optical communication and digital technologies. As the demand for faster, more efficient data transmission grows, photonic crystals have become a key technology in overcoming the limitations faced by traditional electronic and optical systems. This report delves into the fundamental principles of photonic crystals, focusing on how their periodic structures create photonic bandgaps that control the propagation of light. These properties make photonic crystals essential for high-speed data transmission and signal processing. The report also covers the different types of photonic crystals, including 1D, 2D, and 3D structures, highlighting their unique applications in various systems. Furthermore, the report explores the fabrication techniques used to create these complex structures, such as lithography, self-assembly, and advanced nanofabrication. It examines the challenges faced in large-scale production and the material selection required for efficient performance.

In addition, the report investigates the key applications of photonic crystals in optical communication, where they enhance fibre-optic networks, improve signal processing, and enable high-speed data transmission. These advancements are crucial for telecommunication systems that demand low-latency and high-bandwidth capabilities. The integration of photonic crystals into digital technologies is also explored, particularly in the fields of optical computing, quantum computing, and AI, where they enable faster, more energy-efficient processing. The report also addresses the challenges involved in scalability, integration with existing systems, and fabrication complexities. Finally, the report outlines the future prospects of photonic crystals, emphasizing their potential in next-generation technologies. Through these discussions, the report aims to highlight the crucial role of photonic crystal

1.2. FUNDAMENTALS OF PHOTONIC

Photonic crystals are materials with a periodic arrangement of dielectric or metallic structures that manipulate light in ways similar to how atomic lattices influence

electron behaviour in solids. The key feature of photonic crystals is the photonic bandgap (PBG), a phenomenon where specific wavelengths of light are forbidden from propagating through the material, much like how electronic bandgaps prevent electron flow in semiconductors. This ability to control light propagation is due to the periodic arrangement of materials with contrasting refractive indices, which causes light to interact with the crystal in complex ways.

Photonic crystals are classified based on their dimensionality. One-dimensional (1D) photonic crystals consist of alternating layers of materials with different refractive indices, affecting light propagation along one axis. These are often used in applications like optical coatings and filters. Two-dimensional (2D) photonic crystals have periodic structures that extend across two axes, allowing for control over light in two dimensions. They are commonly used in waveguides, sensors, and beam steering devices. Three-dimensional (3D) photonic crystals, where the periodic structure extends in all three spatial directions, offer the most complete control over light. They create a complete photonic bandgap, blocking light across a broad range of frequencies, making them ideal for advanced applications like optical communication and quantum computing.

At the heart of photonic crystals is their ability to form regions where light is either strongly confined or fully blocked, leading to highly efficient control over light propagation, reflection, and transmission. This makes them indispensable in waveguides, resonators, and filters, contributing to the development of faster, more energy-efficient optical communication and computing systems.

1.2.1 Definition and Basic Principles

Photonic crystals are materials with a periodic structure that is designed to manipulate the behavior of light. These structures are analogous to how atomic lattices in semiconductors control electron motion, but in this case, they control the propagation of electromagnetic waves, particularly light. The periodicity of these materials, typically at the scale of the wavelength of light, creates a photonic bandgap (PBG), which is a range of wavelengths where light cannot propagate through the material. This

phenomenon is similar to the electronic bandgap in semiconductors, which determines which energies electrons can or cannot have.

The basic principle behind photonic crystals is their ability to selectively block or allow the propagation of certain wavelengths of light. This selective control over light is achieved through the periodic arrangement of materials with different refractive indices. These periodic structures cause light waves to interact with the material in ways that interfere with their propagation, resulting in the creation of bandgaps where light of certain frequencies cannot pass through.

1.2.2. Comparison with Electronic Band Structures

Photonic crystals and electronic band structures share a fundamental similarity in that both rely on periodic structures to control the flow of energy, either through electrons or photons. In semiconductors, the periodic arrangement of atoms creates electronic bandgaps, which define the allowed and forbidden energy levels for electrons, determining whether a material behaves as a conductor, insulator, or semiconductor. Similarly, photonic crystals create photonic bandgaps (PBGs) through the periodic arrangement of materials with different refractive indices, blocking certain wavelengths of light while allowing others to propagate. This concept of allowed and forbidden states is analogous in both cases, where electrons can only occupy energy levels within the allowed bands, and light can only propagate at wavelengths within the photonic bands. Additionally, while electronic band structures are typically considered in three-dimensional materials, photonic crystals can be engineered in 1D, 2D, or 3D configurations, providing greater flexibility in controlling light propagation. This ability to manipulate light at specific wavelengths is particularly useful for waveguides, filters, and resonators in optical communication and computing systems. Both photonic crystals and electronic materials rely on their respective periodic structures to guide and control energy but in different forms: electrons in the case of semiconductors and photons in the case of photonic crystals. Ultimately, the analogous behaviour of these systems in controlling energy flow has led to advances in both electronic devices and

optical technologies, with photonic crystals offering new possibilities for light-based communication, computing, and photonics-based applications.

1.2.3 Types of Photonic Crystals

1.2.3.1 One-Dimensional (1D) Photonic Crystals

One-dimensional (1D) photonic crystals consist of alternating layers of materials with different refractive indices, creating a periodic structure along one direction. This simple configuration allows for the control of light propagation along a single axis, making 1D photonic crystals ideal for applications such as optical filters, reflectors, and antireflection coatings. Light passing through these structures experiences interference, leading to reflection or transmission of specific wavelengths. The periodicity of the layers can be designed to create narrow photonic bandgaps (PBGs) that block certain wavelengths while allowing others to pass. 1D photonic crystals are often used in devices like multilayer coatings for lasers or optical cavities, where the control of light is primarily needed along one axis.

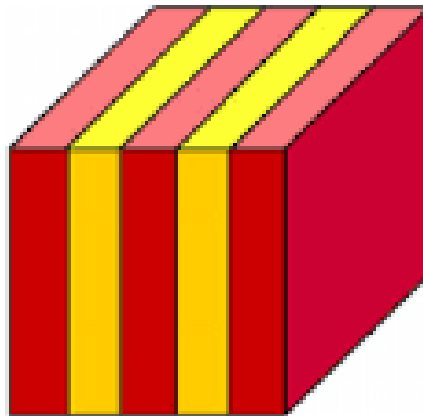


Figure 1.1 One-dimensional (1D) Photonic Crystals

1.2.3.2 Two-Dimensional (2D) Photonic Crystals

Two-dimensional (2D) photonic crystals extend the periodic structure across two dimensions, usually in a plane. These crystals have a periodic arrangement of materials in a 2D lattice, which can manipulate light propagation within the plane of the crystal. The most common example is the square or hexagonal lattice structure. 2D photonic

crystals are widely used in applications such as waveguides, sensors, and beam-steering devices, where control over light in two directions is necessary. By utilizing a 2D photonic crystal, engineers can direct light in a specific path or suppress unwanted modes. These crystals often exhibit complete photonic bandgaps in two dimensions, preventing the propagation of light within a specific range of wavelengths or directions.

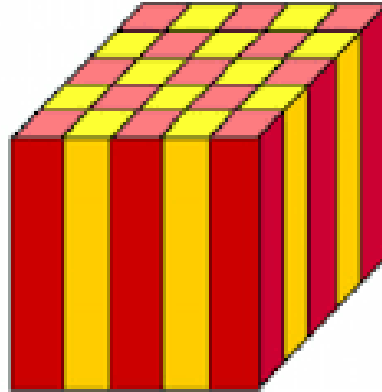


Figure 1.2 Two-dimensional (2D) Photonic Crystals

1.2.3.3 Three-dimensional (3D) Photonic Crystals

Three-dimensional (3D) photonic crystals are the most complex, with periodicity in all three spatial directions. These crystals can create a complete photonic bandgap that blocks the propagation of light in all directions, making them ideal for advanced optical devices that require high precision in controlling light across a broad range of wavelengths. 3D photonic crystals can be used in applications such as optical communication, imaging, and quantum computing, where it is necessary to control light flow completely.

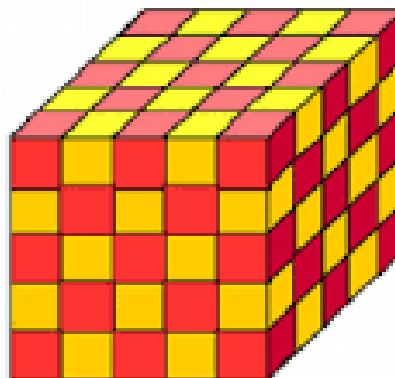


Figure 1.3 Three-dimensional (3D) Photonic Crystals

These structures are challenging to fabricate but offer the highest degree of control over light, enabling innovations in light trapping, superlattices, and photonic circuits.

1.2.3.4 Photonic Bandgaps (PBGs) and Their Significance

Photonic bandgaps (PBGs) are a central feature of photonic crystals, analogous to electronic bandgaps in semiconductors. A PBG is a range of wavelengths (or frequencies) where light cannot propagate through the photonic crystal, similar to how certain electron energies are forbidden in semiconductors. The significance of PBGs lies in their ability to control and manipulate light in highly precise ways. PBGs allow photonic crystals to block or guide light at specific wavelengths, enabling the design of devices with properties such as low-loss waveguiding, inhibition of spontaneous emission, and directional light propagation. By adjusting the structure of the photonic crystal, engineers can tune the size and position of the PBG to target specific wavelengths or frequencies. This capability is crucial for applications in optical communication systems, laser cavities, microsensors, and quantum technologies, where precise control of light is essential.

1.3. FABRICATION TECHNIQUES FOR PHOTONIC CRYSTALS

Fabricating photonic crystals involves several advanced techniques to create periodic structures that control light propagation. One widely used method is photolithography, where a photoresist is applied to a substrate, and light is used to transfer patterns from a mask onto the resist, creating periodic features. Electron beam lithography (e-beam lithography) offers higher precision by directly writing custom patterns onto the resist using an electron beam, making it suitable for small-scale or research purposes. Nanoimprint lithography involves pressing a nanoscale mold onto a resist layer, transferring fine patterns onto the substrate, and is often used for large-scale production due to its high throughput and efficiency. Self-assembly techniques exploit the natural ability of materials like nanoparticles or block copolymers to spontaneously organize into ordered structures, a process that can be guided by external forces like magnetic fields or solvent evaporation, making it suitable for large-scale, cost-effective

fabrication. Finally, direct laser writing uses focused laser beams to create micro or nanostructures directly on a material, offering high resolution and versatility for creating complex photonic crystal designs. Each of these techniques is chosen based on the specific requirements of the photonic crystal, such as resolution, scale, and the material involved.

1.3.1 Lithographic methods (e-beam lithography, nanoimprint lithography)

Lithographic techniques, such as electron beam lithography (e-beam lithography) and nanoimprint lithography, are essential for fabricating photonic crystals with high precision. These methods allow for the creation of fine, periodic structures that control light propagation at subwavelength scales. Below is an overview of these two important lithographic techniques

1.3.1.1 Electron Beam Lithography (e-beam Lithography)

Electron beam lithography is a direct-write technique where an electron beam is used to expose a resist-coated substrate, creating highly detailed patterns. Unlike traditional photolithography which uses masks and UV light, e-beam lithography offers fine resolution and the ability to pattern custom designs without the need for masks.

Process:

1. **Coating:** A substrate (e.g., silicon, glass) is coated with a layer of electron-sensitive resist, such as polymethyl methacrylate (PMMA).
2. **Exposure:** The electron beam is directed onto the resist. The electron beam's energy causes the resist in the exposed regions to either cross-link (positive resist) or degrade (negative resist).
3. **Development:** After exposure, the resist is developed using a solvent. In the case of positive resist, the exposed areas are removed, while in negative resist, the unexposed areas are washed away.
4. **Etching:** The patterned resist serves as a mask for subsequent etching processes that transfer the pattern into the underlying material, such as silicon or a metal layer.

1.3.1.2 Nanoimprint Lithography (NIL)

Nanoimprint lithography is a technique that involves mechanically pressing a mold with nanoscale patterns onto a resist layer to transfer the pattern. It is a high-throughput method, providing a cost-effective alternative to traditional photolithography and e-beam lithography for large-scale production of nanostructures.

Process:

1. **Resist Coating:** A thin layer of resist, such as UV-curable polymers, is coated onto the substrate.
2. **Imprint:** A mold, typically made from materials like silicon or quartz, is pressed into the resist. The mold contains a pre-etched pattern corresponding to the desired photonic crystal structure.
3. **Curing:** The resist is cured, usually by UV light or heat, depending on the resist material. This hardens the resistance in the patterned areas, effectively capturing the mold's structure.
4. **Mold Removal:** After curing, the mold is carefully removed, leaving behind the replicated nanoscale pattern on the substrate.
5. **Etching:** If necessary, an etching step can transfer the pattern from the resistor into the underlying substrate, such as silicon or glass.

1.3.2 Advanced Nanofabrication Methods (3D printing, laser interference lithography)

As the demand for complex and precisely engineered photonic crystals increases, advanced nanofabrication methods such as 3D printing and laser interference lithography have emerged as powerful tools for creating intricate nanoscale structures. These methods offer distinct advantages in terms of scalability, versatility, and precision.

1.3.2.1 3D Printing for Nanofabrication

3D printing, also known as additive manufacturing, is a method where materials are deposited layer by layer to create complex 3D structures. While traditional 3D printing techniques focus on macro-scale structures, advancements in nanoscale 3D printing have enabled the fabrication of photonic crystals and other nanostructures.

Process:

1. **Material Selection:** Nanoscale 3D printing uses materials like resins, nanoparticles, or metal inks. For photonic crystals, specialized materials that exhibit the necessary optical properties are chosen.
2. **Printing:** The material is deposited layer by layer using techniques like **stereolithography (SLA)**, **two-photon polymerisation**, or **fused deposition modeling (FDM)**. In two-photon polymerization, for example, a laser is focused on a resin bath to polymerise the material with extreme precision.
3. **Curing and Post-Processing:** After printing, the structure may be cured or treated with heat or UV light to enhance the mechanical properties or optical performance.
4. **Characterization:** The resulting structures are characterized for optical properties, such as their bandgap behaviour or light manipulation capabilities.

1.3.1.2 Laser Interference Lithography (LIL)

Laser interference lithography is a high-precision technique used to create periodic nanostructures by exploiting the interference pattern generated when two or more coherent laser beams overlap. It is particularly effective for producing large-area photonic crystal patterns with periodicity in the range of hundreds of nanometers to micrometres.

Process:

1. **Laser Setup:** Two or more coherent laser beams (often from a single laser source) are directed at a photosensitive material (e.g., photoresist) on a substrate.

The beams can either interfere at a fixed angle or be directed perpendicularly to each other, depending on the desired pattern.

2. **Interference Pattern:** The interference of the laser beams creates a standing wave pattern of light, where constructive interference leads to areas of high intensity, and destructive interference creates regions of low intensity. This interference pattern defines the periodic structure on the surface of the resist.
3. **Exposure:** The resist material is exposed to this interference pattern, causing it to polymerize or break down, depending on whether a positive or negative resist is used.
4. **Development:** After exposure, the resist is developed, revealing the patterned structure.
5. **Etching:** The exposed pattern can be transferred into the underlying material (e.g., silicon, glass) using etching techniques like reactive ion etching (RIE).

1.3.3 Self-Assembly Techniques for Photonic Crystal Fabrication

Self-assembly techniques are powerful, bottom-up approaches for fabricating photonic crystals without the need for complex lithographic equipment. These methods leverage the natural tendency of materials to organize into periodic structures, making them cost-effective and scalable for large-area applications. Two major self-assembly techniques used for photonic crystal fabrication are colloidal crystallization and block copolymer templating.

1.3.3.1 Colloidal Crystallization

Colloidal crystallization is a self-assembly technique in which monodisperse colloidal particles (e.g., silica or polystyrene spheres) spontaneously organize into highly ordered, periodic structures due to interparticle forces. This method mimics the natural formation of opals, which exhibit photonic bandgap effects due to their periodic arrangement.

Process

1. Preparation of Colloidal Suspension

Monodisperse spherical colloidal particles (100 nm – 1 μ m in diameter) are synthesized using techniques like Stöber synthesis (for silica) or emulsion polymerization (for polystyrene).

2. Self-assembly via Controlled Evaporation or Sedimentation

- The colloidal suspension is deposited onto a substrate.
- As the solvent evaporates, capillary forces drive the particles to arrange into a close-packed, face-centred cubic (FCC) or hexagonal structure.
- Alternatively, gravitational sedimentation can lead to self-organization into ordered colloidal crystals.

3. Fixation and Template Inversion (Optional)

- The assembled colloidal crystal can be used as a **template** to create inverse opal structures.
- A material such as silicon or a polymer is infiltrated into the gaps between the spheres, and the original colloidal template is removed by chemical etching or thermal decomposition.

1.3.3.2 Block Copolymer Templating

Block copolymers (BCPs) are macromolecules composed of two or more chemically distinct polymer blocks that can phase-separate into periodic nanoscale structures. This intrinsic self-organization can be harnessed to create nanoscale photonic crystals, providing sub-100 nm feature sizes.

Process

1. Block Copolymer Selection

- A diblock or triblock copolymer system is chosen (e.g., polystyrene-b-poly(methyl methacrylate) (PS-b-PMMA) or polystyrene-b-polyisoprene (PS-b-PI)).
- The molecular weight and composition of the copolymer dictate the periodicity and structure of the self-assembled domains.

2. **Thin Film Deposition**

- The block copolymer is dissolved in a solvent and spin-coated onto a substrate, forming a thin film.

3. **Template Inversion and Etching**

- One polymer phase is selectively removed (e.g., by reactive ion etching or UV degradation), leaving behind a porous template.
- The voids can be filled with materials such as silicon or metals to fabricate inverse structures.

CHAPTER 2

LITERATURE SURVEY

Bing Qing Zhu and Hon Ki Tsang (2016) presented a high coupling efficiency mode converter for transitioning between silicon waveguides and metal-insulator-metal (MIM) waveguides. The proposed device addresses the challenge of efficient coupling between low-loss silicon photonics and plasmonic waveguides, which are known for their subwavelength confinement. The design leverages a tapered waveguide structure to minimize mode mismatch and optimize energy transfer. Numerical simulations evaluate the converter's performance, focusing on metrics such as coupling efficiency, insertion loss, and bandwidth.

Islam et al. (2025) investigated the lattice structure-dependent modulation of the photonic band gap (PBG) in gallium phosphide (GaP)-based 2D photonic crystals. The study explores how variations in the lattice geometry of the photonic crystal can influence the PBG, which is critical for controlling light propagation and guiding in photonic devices. The researchers focus on the design of 2D photonic crystals made from GaP, a material known for its excellent optical properties. Using numerical simulations, the study analyzes the effect of different lattice structures (e.g., hexagonal, square) on the photonic band gap, investigating the relationship between lattice geometry, band gap width, and material properties.

Fan et al. (2025) presented a study on optically tunable terahertz metamaterials fabricated on highly flexible substrates. This work explores the development of metamaterials that exhibit tunable terahertz (THz) properties, offering potential applications in THz imaging, sensing, and communication systems. The proposed metamaterials incorporate optically responsive materials that allow the manipulation of the material's properties using light. These metamaterials are designed to be integrated onto flexible substrates, making them suitable for wearable electronics, flexible sensors, and conformal THz devices. The study uses both experimental and numerical methods to characterize the tuning mechanisms and performance metrics such as resonance shift, transmission, and modulation depth in the THz frequency range.

Malhotra, Liu, and Mi (2025) presented a study on the design principles and performance limitations of InGaN nanowire photonic crystal micro-LEDs. The paper explored the integration of indium gallium nitride (InGaN) nanowires with photonic crystal structures to enhance the performance of micro-LEDs, particularly in the context of efficient light emission, optical confinement, and device scalability. The study delves into the design guidelines for optimizing the micro-LED structure, including the dimensions and arrangement of nanowires and the photonic crystal lattice. The authors also examine the performance limitations imposed by factors such as material defects, light extraction efficiency, and optical losses within the nanowire-based micro-LEDs.

Khan et al. (2025) proposed a highly compact split ring resonator-based rectangular dielectric resonator antenna (DRA) with multiband characterization. The study focuses on the design of a compact antenna that utilizes split ring resonators (SRRs) integrated with a dielectric resonator for enhanced performance in multiband applications. The antenna design incorporates SRRs to achieve multiple resonance frequencies, allowing the antenna to operate efficiently across different bands. The study uses electromagnetic simulations to analyze the antenna's performance in terms of resonance frequency, impedance matching, and radiation patterns. Key characteristics such as size reduction, bandwidth enhancement, and radiation efficiency are evaluated to optimize the overall performance of the antenna.

Wei et al. (2025) presented a practical and accurate evaluation of the numerical aperture (NA) and beam quality factor (BQF) in photonic crystal fibers (PCFs) using mechanical learning techniques. The study focused on improving the assessment of optical properties in PCFs, which are crucial for a variety of applications, including high-precision sensing and communication systems. The research introduces a mechanical learning-based approach to model and evaluate the NA and BQF of PCFs, overcoming the limitations of traditional analytical methods.

Dong et al. (2025) explored the generation of ultraviolet-enhanced flat supercontinuum light in cascaded photonic crystal fibers (PCFs). The study focuses on advancing the generation of supercontinuum light across a broad spectrum by using the

unique properties of PCFs, which offer high flexibility in controlling light propagation and dispersion. The authors propose a cascaded PCF configuration that enhances the supercontinuum generation process, specifically improving the ultraviolet (UV) region of the spectrum. By optimizing the fiber design and utilizing the nonlinear optical effects in the cascaded structure, the researchers are able to generate a flat supercontinuum spectrum, extending into the ultraviolet range with high efficiency.

Varshney et al. (2025) presented a comprehensive study on the characterization of effective parameters and circuit modeling of a U-coupled hybrid ring resonator band pass filter. This work focuses on improving the performance of band pass filters used in microwave and RF circuits by introducing a novel U-coupled hybrid ring resonator design that optimizes filter characteristics such as bandwidth, selectivity, and frequency response. The authors develop a circuit model for the U-coupled hybrid ring resonator, which incorporates key parameters such as coupling coefficients, resonator Q-factors, and frequency shifts. The study uses electromagnetic simulations and experimental measurements to validate the proposed model and evaluate the filter's performance across various frequency ranges.

Mateus I. O. Souza et al. (2025) investigated microwave glucose sensing using double circular split ring resonators (DCSRRs) to improve sensitivity in glucose detection. The study focuses on the development of a highly sensitive sensor that can be used for non-invasive glucose monitoring, which is particularly relevant for diabetes management and healthcare applications. The authors propose the use of DCSRRs to enhance the sensor's performance, leveraging the resonant properties of the split ring resonators to achieve higher sensitivity to glucose concentration changes. The study examines the influence of different substances, such as artificial blood plasma and deionized water, on the sensor's performance to better understand how biological fluids impact the detection process.

Kola Thirupathaiah and Montasir Qasymeh (2023) proposed an optical ultra-wideband nano-plasmonic bandpass filter based on gap-coupled square ring resonators. This study aims to develop a highly efficient bandpass filter that operates in the optical

range, particularly targeting ultra-wideband (UWB) applications with an emphasis on nano-plasmonics. The authors introduce gap-coupled square ring resonators as a promising approach for achieving high-performance optical filtering. The design leverages the unique properties of plasmonic resonators to create a narrowband resonance while maintaining an ultra-wide transmission window. The study presents a detailed analysis of the optical transmission characteristics, resonant frequencies, and performance metrics of the filter, highlighting its potential for use in optical communication and sensing applications.

Shiqi He et al. (2023) presented an analytic theory for parametric amplification in high-Q micro-ring resonators. The study focuses on enhancing the performance of micro-ring resonators by utilizing parametric amplification, which can significantly improve signal amplification in optical communication systems and other high-frequency applications. The authors derive a theoretical framework that models the behaviour of parametric amplification in high-Q micro-ring resonators, considering factors such as pump power, signal gain, and the impact of nonlinear interactions in the resonator structure. The analysis provides valuable insights into the conditions necessary for effective amplification and the optimization of micro-ring resonators for high-performance applications.

Agilandeswari et al. (2022) proposed a highly integrated and reconfigurable platform for Photonic Integrated Circuits (PICs) using coupled nanoring resonators. This novel structure enables the realization of multiple optical components—including a wavelength multiplexer, D-flip flop, power splitter, reconfigurable switch, and bandpass filter—within a single compact device. Using the Finite-Difference Time-Domain (FDTD) method for analysis, the authors demonstrated impressive performance metrics such as a data rate of 5.4 Tbps, an ON-OFF ratio of 36.98 dB, ultra-compact area of $186.48 \mu\text{m}^2$, and very low insertion loss (0.0043 dB). The multifunctional capability of this design reduces the footprint, cost, and power requirements, making it ideal for scalable optical computing, photonic communication systems, and optical interconnects. The study also reviews existing multifunctional photonic platforms, including those utilizing graphene-integrated waveguides, Mach-

Zehnder Interferometers (MZI), and photonic crystal-based devices. Compared to prior works, the coupled nanoring structure presents a highly compact and efficient alternative for next-generation photonic technologies.

Geerthana et al. (2023) present a novel design for a chain-shaped photonic crystal-based ring resonator (PhCRR) that functions as a channel drop filter (CDF) for coarse wavelength division multiplexing (CWDM) applications. This design utilizes two-dimensional photonic crystals (2D-PhCs), where silicon rods with a refractive index of 3.44 are perforated in air with a refractive index of 1. The choice of silicon is crucial due to its nearly zero absorption in the C-band (1530–1565 nm), making it ideal for low-loss optical components. The PhCRR structure is designed within two-dimensional hexagonal lattices, which provide a well-defined photonic band gap. The key performance metrics of the proposed resonator include a high transmission efficiency of 99.7%, a quality factor (Q-factor) of 4550 at a wavelength of 1551 nm, and minimal loss (less than 0.2 dB).

Ishimura et al. (2023) proposed and demonstrate free-space optical communication using photonic crystal surface-emitting lasers (PCSELs). The study focuses on the application of PCSELs as a new light source for free-space optical communication (FSO), aiming to overcome the limitations of traditional communication systems, such as signal attenuation and interference in the atmosphere. The authors explore the advantages of PCSELs, such as their narrow emission angles, high optical power, and wavelength tunability, which make them ideal for long-range, high-bandwidth FSO systems. The study provides both theoretical analysis and experimental demonstration of how PCSELs can be used to establish high-performance optical links in free-space environments.

Rafi et al. (2023) presented a wideband tunable modified split-ring resonator (SRR) structure, leveraging liquid metal and 3D printing technologies. The innovative approach seeks to address limitations in traditional SRR-based devices by introducing dynamic tunability, allowing the resonator to adjust its resonance frequency across a wide range. The use of liquid metal enables this flexibility, as it allows for real-time

changes in the physical structure of the resonator, offering a broad operational bandwidth ideal for microwave applications.

Rajasekar et al. (2023) presented a numerical analysis of a reconfigurable and multifunctional photonic crystal ring resonator (PCRR) platform based on barium titanate (BaTiO_3). The platform exploits the high electro-optic and nonlinear optical properties of BaTiO_3 to achieve dynamic control over optical signal processing functions. The proposed PCRR design integrates barium titanate as the core material, enabling tunable resonance characteristics through an applied electric field. The study examines critical performance metrics, including resonance wavelength tunability, quality factor, and optical confinement. The multifunctional nature of the platform supports applications.

Sharma et al. (2023) explore a photonic crystal-based biosensor for the detection of cancer cells, utilizing the finite-difference time-domain (FDTD) method for numerical analysis. The proposed biosensor leverages the sensitivity of photonic crystals to refractive index variations, enabling precise detection of cancer biomarkers. The design features a 2D photonic crystal structure with a defect region engineered to trap and guide light. The authors investigate the sensor's performance by analyzing parameters such as the resonance wavelength shift and sensitivity. Cancer cell detection is facilitated through changes in the refractive index caused by the presence of cancerous biological material in the analyte.

Sharma (2023) presented the analysis and design of a photonic crystal-based biochip for the detection of glycosuria (the presence of glucose in urine). The proposed biochip utilizes the optical properties of photonic crystals to identify changes in the refractive index caused by glucose molecules in the sample. The biochip design incorporates a 2D photonic crystal structure with a central defect region that enhances light-matter interaction. Numerical simulations analyze the sensor's performance, focusing on parameters such as sensitivity, quality factor, and resonance wavelength shift.

Rajasekar et al. (2022) presented a numerical investigation of a reconfigurable photonic crystal switch utilizing phase-change nanomaterials. The proposed design leverages the unique properties of phase-change materials to achieve dynamic switching of optical signals within a photonic crystal structure. The study employs numerical simulations to analyze the switching performance, focusing on key parameters such as insertion loss, extinction ratio, and switching speed. The integration of the phase-change nanomaterial enables the switch to operate between amorphous and crystalline states, providing high contrast in refractive index. This reconfigurability enhances the efficiency and flexibility of the switch.

Jovana Nojić et al. (2021) investigated laser phase noise in ring resonator-assisted direct detection data transmission. This study addresses the impact of laser phase noise on the performance of direct detection systems that use ring resonators, which are integral components in optical communication systems. The authors focus on understanding how laser phase noise affects signal quality and data transmission accuracy in systems that utilize ring resonators for direct detection. They provide a detailed analysis of the noise characteristics and derive mathematical models to predict its influence on the system's signal-to-noise ratio (SNR) and overall performance.

Nandhini V L. et al. (2020) proposed a novel waveguide resonator-based optical sensor for the detection of vitiligo, a skin condition characterized by the loss of pigmentation. The design utilizes the sensitivity of optical waveguide resonators to refractive index changes, enabling early-stage detection of vitiligo by identifying alterations in skin tissue properties. The waveguide resonator structure is optimized to enhance light-matter interaction, with the sensor capable of detecting the slight refractive index changes associated with vitiligo. The study focuses on the sensitivity, detection limit, and resonance shift when exposed to skin samples exhibiting vitiligo.

Arunkumar et al. (2019) presented the design and analysis of a 2D photonic crystal-based biosensor for detecting different blood components. The sensor leverages the high sensitivity of photonic crystals to variations in the refractive index, enabling accurate identification of specific blood components. The proposed biosensor features

a square lattice photonic crystal structure with a central defect engineered to guide light. Using numerical simulations, the authors analyze the device's performance in terms of resonance wavelength shift, sensitivity, and quality factor. Each blood component, characterized by its unique refractive index, causes a distinct resonance shift.

Rashki and Chabok (2018) propose a novel design for photonic crystal ring resonator-based optical channel drop filters. The study focuses on developing a compact and efficient structure for filtering specific optical channels in wavelength-division multiplexing (WDM) systems. The proposed design utilizes photonic crystal ring resonators (PCRRs) integrated into a 2D photonic crystal lattice. The PCRRs are optimized to achieve high-quality filtering with minimal insertion loss. The device performance is analyzed based on parameters such as resonance wavelength, quality factor, and transmission efficiency.

Shen et al. (2013) investigated an ultra-compact integration of a photonic crystal (PC) splitter and a slow-light waveguide for a microwave photonic filter. Their approach leveraged the slow-light effect in a photonic crystal waveguide to achieve a compact filter design with a free spectral range (FSR) of 130 GHz and a notch depth of 10 dB. The filter, with a total length of only 24.8 μm , was implemented using a U-shaped waveguide, which enhanced integration density. Additionally, an optimized linear taper structure was introduced to improve coupling efficiency from 10% to 62%. This work demonstrates the potential of photonic crystal-based waveguides in high-frequency applications such as 60-GHz Radio-over-Fiber (RoF) systems, offering advantages in footprint reduction and signal processing efficiency.

Akowuah et al. (2012) present a numerical analysis of a photonic crystal fibre (PCF) design for biosensing applications. The PCF structure is optimized to enhance light-matter interaction, enabling high sensitivity for detecting biological analytes. The study uses finite element modelling to simulate light propagation and identify key optical properties such as mode field distribution and confinement loss. The design features air holes in a hexagonal lattice, with a central defect to guide light. By carefully tuning the PCF parameters, the authors achieved a high degree of confinement and

improved sensitivity for refractive index changes in the surrounding medium. The reported sensitivity reached values as high as 10,000 nm/RIU, making it a promising platform for real-time biological sensing. This work demonstrates the potential of PCFs in label-free biosensing and highlights their suitability for applications in healthcare, environmental monitoring, and biochemical analysis.

CHAPTER 3

EXISTING METHOD

3.1 INTRODUCTION

Light-based technology outperforms other fields due to its miniature structure, low power consumption, and high bandwidth. Photonic crystals (PhCs) have gained attention for designing optical devices like filters, modulators, and photonic integrated circuits (PICs). Optical filters are crucial in optical add-drop multiplexers (OADMs) and other optical systems. PhC-based ring resonators (PhCRRs) are compact and flexible, making them ideal for various applications, including wavelength selectors, multiplexers, and logic gates. PhCRRs typically consist of bus and drop waveguides with a ring resonator in between. Researchers have developed different resonator configurations, such as sidewall and top grating-based structures, achieving high Q-factors and efficiency. The resonant wavelength of a PhCRR can be adjusted by modifying the ring's core radius, refractive index, and shape. Various PhCRR geometries, including square, circular, and hexagonal, have been explored, but existing designs exhibit low quality factors (<1000) and moderate efficiencies (80–90%). This study introduces a novel chain-shaped PhCRR with improved transmission efficiency and Q-factor. The paper covers the mathematical modeling, structural design, and numerical analysis of the proposed PhCRR, demonstrating its superior performance compared to existing models.

3.2 DEFINITION

This study presents a chain-shaped photonic crystal-based ring resonator (PhCRR) designed as a channel drop filter (CDF) using two-dimensional photonic crystals. The structure consists of silicon rods (refractive index 3.44) embedded in air (refractive index 1) within a hexagonal lattice. Silicon is chosen for its minimal absorption in the C-band (1530–1565 nm). The proposed PhCRR achieves a high transmission efficiency of 99.7% and a quality factor of 4550 at a wavelength of 1551 nm. The functionality of the drop filter is analyzed by calculating the electric field distribution at 1551 nm and

1553 nm. Simulation results are obtained using the finite-difference time-domain (FDTD) numerical analyzer, while the plane wave expansion solver method is used to estimate the photonic band gap. Operating in the third optical window with a low loss of less than 0.2 dB, the designed PhCRR is suitable for applications in tunable add/drop multiplexing, optical filtering, signal routing, CWDM systems, free-space communication, and photonic integrated circuits. This research highlights the potential of PhCRRs in achieving high-performance optical filtering with improved transmission efficiency and quality factor.

3.3 RING RESONATOR

3.3.1 Square and quasi-square-shape PCRR

Square and quasi-square shaped photonic crystal ring resonators (PhCRRs) are widely used in optical communication and signal processing due to their ability to confine and manipulate light effectively. A square-shaped PhCRR consists of a ring resonator arranged in a perfect square configuration, typically formed using periodic dielectric rods or air holes in a photonic crystal structure. This design ensures strong light confinement, compactness, high transmission efficiency, and tunable resonance, making it suitable for applications such as optical filtering in WDM systems, wavelength-selective switches, and biosensors. However, sharp corners in the square shape can lead to higher transmission loss due to scattering effects. To overcome these limitations, a quasi-square PhCRR is designed with slight modifications, such as rounded or angled edges, to optimize performance. This structure enhances the quality factor (Q-factor) by reducing scattering loss, improves coupling efficiency, and achieves lower transmission loss compared to a conventional square PhCRR. Due to these advantages, quasi-square PhCRRs are preferred in high-Q optical filters, nonlinear optics, and quantum communication applications. While square PhCRRs are simpler in design, quasi-square configurations offer superior performance with

slightly increased design complexity. Both structures play a crucial role in advancing photonic integrated circuits (PICs) and optical signal processing technologies.



Figure 3.1 Square and quasi-square-shape PCRR

3.3.2 Dual curved-shape PCRR

A dual curved-shaped photonic crystal ring resonator (PhCRR) is a specialized resonator design that incorporates two curved sections to enhance optical performance. Unlike traditional square or circular PhCRRs, the dual-curved structure provides improved light confinement and optimized coupling efficiency between the waveguides and the resonator. This unique geometry helps reduce scattering losses and enhances the quality factor (Q-factor), making it suitable for high-performance optical filtering and signal processing applications. The dual-curved PhCRR is typically constructed using two-dimensional photonic crystals with periodic dielectric rods or air holes embedded in a low-index medium. The curvature of the resonator enables better resonance tuning, allowing precise control over the resonant wavelength by adjusting parameters such as refractive index, rod radius, and lattice constant. This design achieves high transmission efficiency with minimal losses, making it ideal for applications in wavelength-division multiplexing (WDM), optical switching, and photonic integrated circuits (PICs). Additionally, the structure supports enhanced nonlinear effects, which can be beneficial for all-optical signal processing and sensing applications. The dual curved-shaped PhCRR provides a balance between compactness, high Q-factor, and improved light-matter interaction,

making it a promising candidate for next-generation optical communication and integrated photonic systems.



Figure 3.2 Dual curved-shape PCRR

3.3.3 Hexagonal-shape PCRR

A hexagonal-shaped photonic crystal ring resonator (PhCRR) is a compact and efficient optical resonator designed using a hexagonal lattice of photonic crystals. This structure is preferred due to its symmetrical geometry, which enhances light confinement, minimizes transmission loss, and improves coupling efficiency. The hexagonal shape offers a balance between compact design and high-quality optical performance, making it an excellent choice for photonic integrated circuits (PICs) and optical communication systems. In a hexagonal PhCRR, the resonator is formed by arranging dielectric rods or air holes in a two-dimensional photonic crystal lattice. The hexagonal symmetry allows for strong optical confinement within the resonator, leading to a higher quality factor (Q-factor) and improved transmission efficiency. By modifying key parameters such as refractive index, rod radius, and lattice spacing, the resonant wavelength can be precisely tuned for specific applications. This structure supports multi-wavelength operation, making it suitable for applications such as optical filtering, wavelength division multiplexing (WDM), biosensing, and optical switching. Compared to square or circular PhCRRs, the hexagonal design provides better field distribution and enhanced spectral selectivity, reducing scattering losses and improving overall device performance. Due to these advantages, hexagonal PhCRRs are widely researched for

next-generation optical communication, signal processing, and sensing applications.



Figure 3.3 Hexagonal-shape PCRR

3.3.4 45-deg-square shape PCRR

A 45-degree square-shaped photonic crystal ring resonator (PhCRR) is a modified square resonator where the structure is rotated by 45 degrees, creating a diamond-like orientation within the photonic crystal lattice. This unique configuration enhances light confinement, reduces transmission loss, and improves coupling efficiency compared to conventional square PhCRRs. The 45-degree rotation alters the optical path, optimizing the interaction between the resonator and the surrounding waveguides, leading to improved resonance characteristics. In this design, dielectric rods or air holes are arranged in a two-dimensional photonic crystal lattice, forming a square ring resonator that is tilted by 45 degrees relative to the waveguides. This orientation minimizes scattering losses at the corners and enhances the quality factor (Q-factor), making it suitable for high-performance optical filtering, wavelength division multiplexing (WDM), and photonic integrated circuits (PICs). Additionally, the rotated structure provides better mode confinement and allows for more precise tuning of the resonant wavelength by adjusting parameters such as rod radius, refractive index, and lattice spacing. Compared to traditional square or quasi-square PhCRRs, the 45-degree square PhCRR offers a balance between compact design, high

transmission efficiency, and low loss, making it an ideal candidate for optical switching, signal processing, and sensing applications in modern photonic networks.

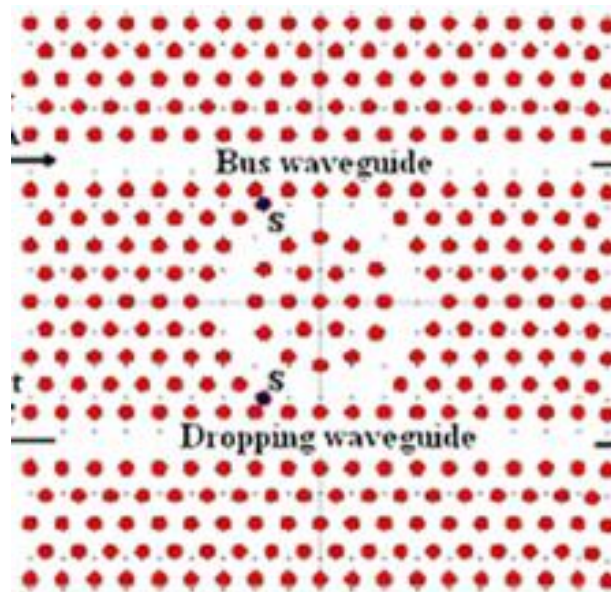


Figure 3.4 45-deg-square shape PCRR

3.3.5 Diamond Shape PCRR

A diamond-shaped photonic crystal ring resonator (PhCRR) is a specialized optical resonator where the ring structure is arranged in a diamond-like configuration within a photonic crystal lattice. This geometry is essentially a 45-degree rotated square PhCRR, optimizing light confinement and improving coupling efficiency between waveguides. The diamond shape helps reduce scattering losses at the corners, leading to an improved quality factor (Q-factor) and enhanced transmission efficiency. The diamond PhCRR is typically designed using two-dimensional photonic crystals (2D PhCs) with a periodic arrangement of dielectric rods or air holes embedded in a low-index medium. The tilted structure enhances field distribution and allows for better resonance tuning by modifying parameters such as refractive index, rod radius, and lattice spacing. Due to its ability to support a high-Q resonance with low transmission loss, this design is widely used in optical filters, wavelength division multiplexing (WDM) systems, biosensors, and photonic integrated circuits (PICs). Compared to square or circular PhCRRs, the diamond-shaped PhCRR provides

enhanced spectral selectivity and more efficient light trapping, making it highly suitable for high-performance optical switching, signal processing, and sensing applications. Its unique geometry allows for greater flexibility in optical design, enabling advancements in next-generation photonic communication systems.

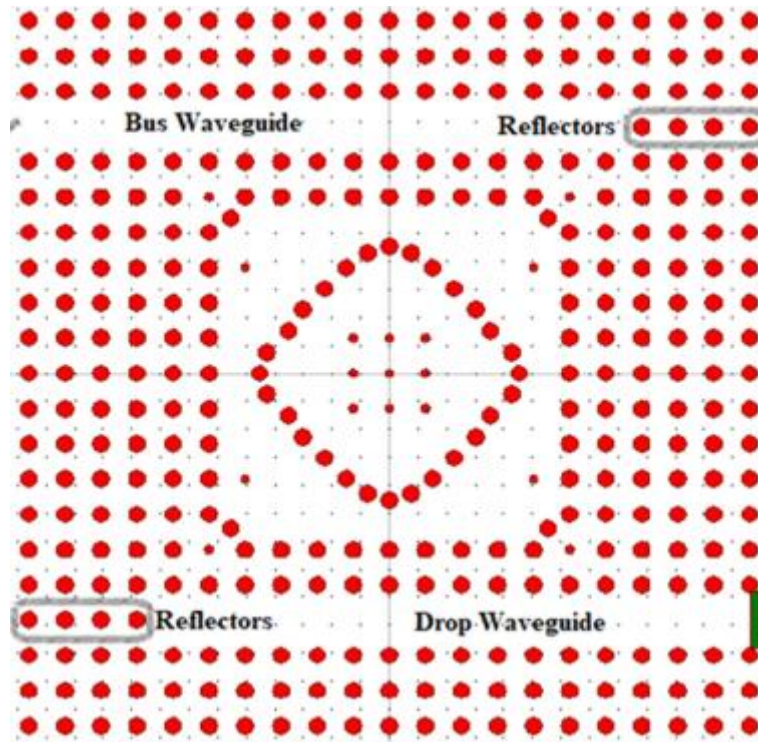


Figure 3.5 Diamond-shape PCRR

3.3.6 X-shape PCRR

An X-shaped photonic crystal ring resonator (PhCRR) is a novel design where the ring resonator is structured in an X-like configuration within a photonic crystal lattice. This unique shape enhances light confinement, improves coupling efficiency, and reduces transmission losses by optimizing the interaction between the resonator and the surrounding waveguides. The X-structure allows for multiple resonance paths, making it particularly suitable for applications requiring multi-wavelength filtering and high-Q resonance performance. The X-shaped PhCRR is typically built using two-dimensional photonic crystals (2D PhCs), where dielectric rods or air holes are periodically arranged to form the resonator. This geometry provides strong mode confinement, enabling a high-quality factor (Q-factor) with minimal optical loss. Additionally, the X-shape offers enhanced spectral selectivity and can be tailored by adjusting parameters such as

rod radius, refractive index, and lattice spacing. This flexibility makes it ideal for optical filtering, wavelength division multiplexing (WDM), optical switching, and biosensing applications. Compared to conventional square, circular, or hexagonal PhCRRs, the X-shaped PhCRR provides better resonance control, increased transmission efficiency, and improved nonlinear optical effects. These advantages make it a promising candidate for high-performance photonic integrated circuits (PICs), free-space optical communication, and advanced signal processing applications in modern optical networks.



Figure 3.6 X-shape PCRR

3.4 Structure of Photonic Crystal Ring Resonator (PhCRR):

A Photonic Crystal Ring Resonator (PhCRR) is an advanced optical component designed using photonic crystals (PhCs), which are periodic dielectric structures that manipulate light propagation by creating photonic bandgaps. These bandgaps allow specific wavelengths to be selectively filtered or confined, making PhCRRs an essential part of modern optical communication and signal processing systems. The proposed PhCRR consists of silicon rods embedded in an air medium, forming a two-dimensional hexagonal lattice. This periodic arrangement ensures that certain wavelengths cannot propagate freely, enabling efficient light confinement and filtering. The hexagonal

lattice structure is chosen because it provides a larger photonic bandgap (PBG) and improved optical performance compared to traditional square or rectangular lattices.

The main components of the PhCRR structure include:

- **Bus Waveguide:** A primary straight waveguide that carries the input optical signal.
- **Drop Waveguide:** A secondary waveguide that extracts specific resonant wavelengths from the ring.
- **Resonant Ring:** A specially designed chain-shaped structure that selectively traps and filters specific wavelengths based on resonance.
- **Input and Output Ports:** The PhCRR is designed with four ports (A, B, C, and D). Ports A and B serve as input ports, while Ports C and D function as output ports for forward and backward wavelength dropping.

The PhCRR is fabricated using silicon rods with a refractive index of 3.44, embedded in an air background with a refractive index of 1. The lattice constant (a) is set to $0.9\ \mu\text{m}$, and the rod radius (r) is defined as $0.29 \times a$ ($0.29\ \mu\text{m}$). The fabrication process involves selectively removing specific silicon rods to introduce line defects that form the bus and drop waveguides. Additionally, point defects are introduced to construct the ring resonator, ensuring minimal optical loss and efficient signal transmission. By carefully selecting design parameters such as lattice spacing and rod radius, the PhCRR structure is optimized to achieve maximum transmission efficiency and a high-quality factor (Q-factor). The photonic bandgap of the structure ensures that only specific wavelengths resonate within the ring, while non-resonant wavelengths continue propagating through the bus waveguide without being affected. The hexagonal lattice configuration offers several advantages, including strong light confinement, reduced scattering losses, and improved optical coupling. This structural optimization makes the PhCRR highly suitable for optical filtering, wavelength-division multiplexing (WDM), signal routing, and photonic integrated circuits (PICs).

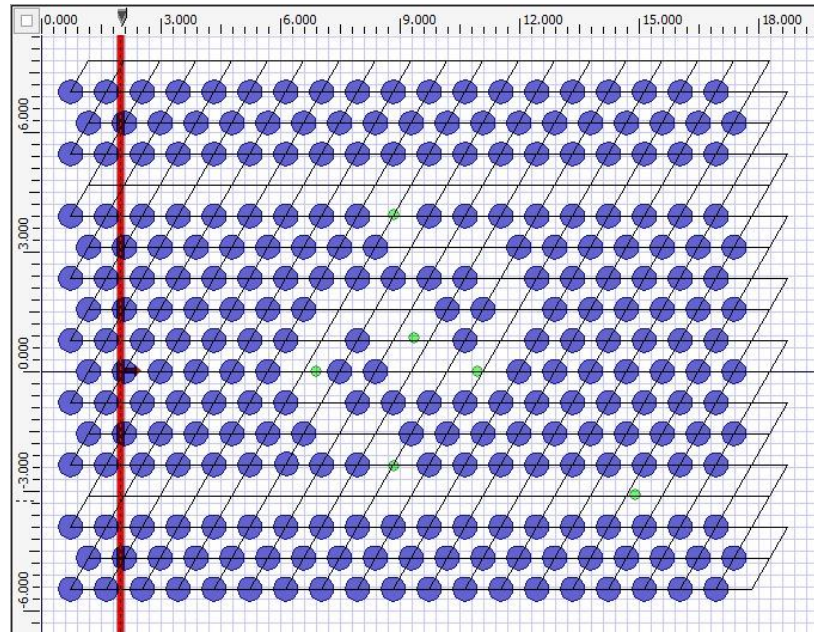


Figure 3.7 Structure of Photonic Crystal Ring Resonator (PhCRR)

3.5 Working Principle of Photonic Crystal Ring Resonator (PhCRR)

The Photonic Crystal Ring Resonator (PhCRR) operates based on the principle of resonant wavelength coupling, enabling selective filtering of optical signals. When an optical signal enters the bus waveguide (Port A or B), certain wavelengths that match the resonance condition of the chain-shaped ring resonator couple into the resonator. These wavelengths circulate within the ring due to multiple internal reflections, while non-resonant wavelengths continue through the bus waveguide unaffected. The PhCRR is designed to function as a channel drop filter (CDF), where specific wavelengths of light are dropped into the drop waveguide (Port C or D) while others continue their path. This filtering occurs due to constructive and destructive **interference** within the ring, where only the resonant wavelengths are efficiently transferred to the drop waveguide.

Resonance Condition and Wavelength Tuning:

The resonant wavelength of the PhCRR is determined by factors such as:

- Lattice constant (a)
- Refractive index of the dielectric material

- Rod radius (r)
- Waveguide coupling efficiency

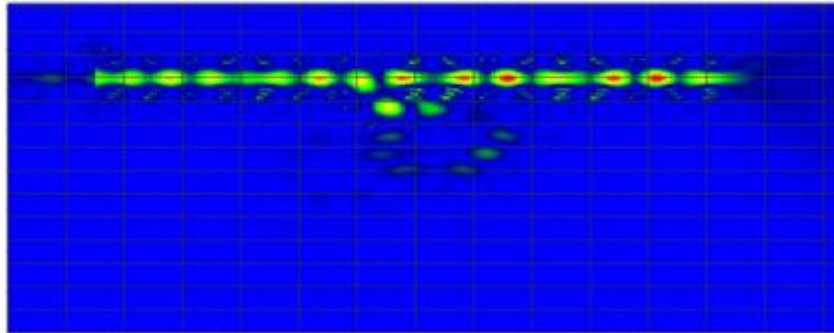


Figure 3.8 Wavelength of 1.57μm

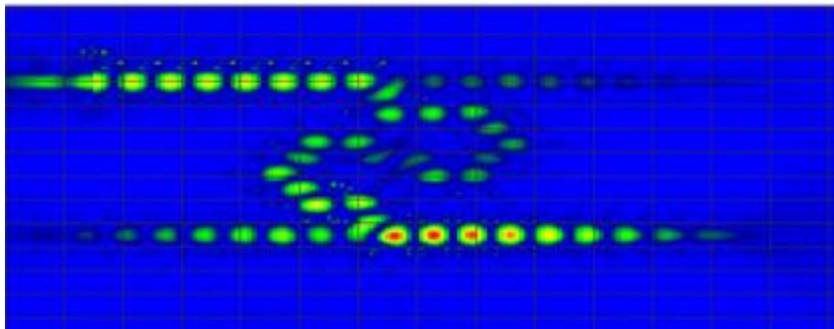


Figure 3.9 Wavelength of 1.53μm

By adjusting these parameters, the resonance condition can be fine-tuned, allowing for precise wavelength selection. This tunability is crucial for applications such as Wavelength-Division Multiplexing (WDM), optical signal processing, and photonic integrated circuits (PICs).

To evaluate the performance of the PhCRR, a Finite-Difference Time-Domain (FDTD) numerical analysis is conducted using Opti-FDTD simulation software. This simulation method helps solve Maxwell's equations, providing insights into the electric field distribution and power transmission characteristics of the resonator. The designed PhCRR achieves a high transmission efficiency of 99.7% with a Q-factor of 4550 at a resonance wavelength of 1551 nm. This high Q-factor indicates excellent optical confinement and minimal energy loss, making the PhCRR highly efficient for real-world applications. Additionally, the structure exhibits a low insertion loss of less than 0.2 dB, further enhancing its performance.

Operational Mechanism:

1. When an optical signal enters the bus waveguide, it travels without significant attenuation.
2. If a specific wavelength matches the resonance condition of the PhCRR, it gets trapped within the ring resonator and circulates due to internal reflections.
3. The resonant wavelength is efficiently coupled into the drop waveguide, exiting through Port C or D, while all other wavelengths continue their journey through the bus waveguide.
4. The efficiency of this dropping mechanism is evaluated by observing the power values at Ports B, C, and D.

Applications and Use Cases:

Due to its ability to selectively filter wavelengths, the PhCRR is widely used in:

- Optical communication systems (WDM, CWDM).
- Photonic integrated circuits (PICs) for signal processing.
- Biosensing applications (detecting small refractive index changes).
- Quantum computing and optical logic gates.

The high Q-factor, tunability, and low-loss characteristics of the PhCRR make it a highly efficient and scalable solution for modern photonic technologies.

CHAPTER 4

PROPOSED METHOD

This project presents a novel approach to wavelength-selective optical signal routing by utilizing a photonic crystal-based add-drop ring resonator, designed and simulated using Finite-Difference Time-Domain (FDTD) techniques in OptiFDTD software. The proposed method exploits the photonic bandgap (PBG) properties inherent in two-dimensional (2D) photonic crystal (PhC) structures to achieve strong light confinement, low-loss transmission, and high spectral resolution. This makes it highly suitable for integrated optical communication systems, particularly for Wavelength Division Multiplexing (WDM) applications.

4.1 Structure Design

The structural foundation of the proposed device is based on a two-dimensional photonic crystal lattice. The PhC comprises a square array of air holes periodically etched into a high-refractive-index silicon substrate, where silicon has a refractive index (n) of approximately 3.46 in the telecommunication wavelength range.

A ring resonator is formed by introducing a loop-shaped defect within the regular lattice. This defect acts as a resonant cavity, enabling light of specific wavelengths to circulate within the closed loop path.

Photonic Crystal-Based Ring Resonator (PhCRR) Device

The Photonic Crystal-Based Ring Resonator (PhCRR) is a compact and highly efficient optical device that typically comprises two straight waveguides — a bus waveguide and a drop waveguide — with a ring-shaped resonator positioned between them. This configuration allows for the selective routing of specific wavelengths from the bus to the drop waveguide, making it ideal for filtering and wavelength-selective applications.

PhCRRs leverage the unique properties of photonic crystals, such as strong light confinement and photonic bandgap engineering, to achieve precise control over light

propagation. When a light signal travels through the bus waveguide, only the resonant wavelength — which matches the ring's optical path length — is coupled into the resonator and dropped to the drop waveguide. Non-resonant wavelengths pass through unaffected.

The resonant wavelength of the PhCRR can be finely tuned by altering parameters such as the core radius, refractive index, geometric shape, and dimensions of the ring. Various resonator shapes have been explored in research, including quasi-square, plus-shaped, hexagonal, rectangular, diamond, circular, dual curve, modified hexagonal, X-shaped, and line defect cavities. Each offers different trade-offs in terms of quality factor (Q-factor) and transmission efficiency.

Despite the versatility of existing designs, many conventional PhCRR structures offer Q-factors below 1000 and conduction efficiencies around 80%–90%. To overcome this limitation, a novel chain-shaped PhCRR has been designed in this work. The proposed structure integrates four ports (Input, Through, Drop, and Add), offering enhanced control over wavelength routing.

Our chain-shaped resonator configuration, inspired by insights from the literature, achieves high transmission efficiency and a significantly improved Q-factor, confirming that complex resonator geometries lead to better performance. The structure's performance has been thoroughly analyzed for various rod radii and

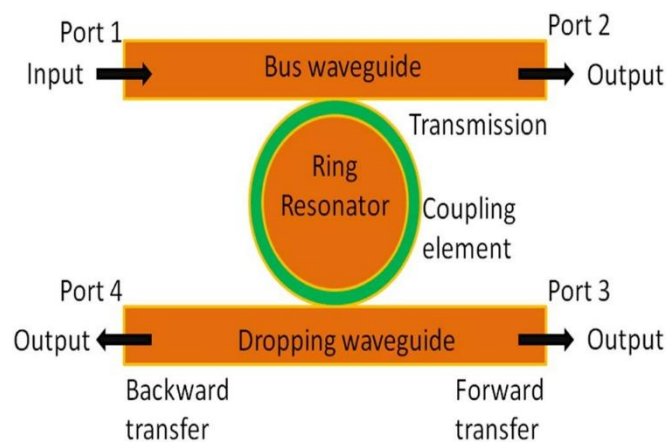


Figure 4.1 Schematic of the basic ring resonator structure with an input port and 3 output ports.

operating wavelengths, demonstrating its robustness and potential for integrated photonic circuits and advanced optical communication systems.

The structure incorporates four essential ports:

- Input Port – where the multi-wavelength signal is introduced into the system.
- Through Port – where wavelengths that do not meet the resonant condition exit the device.
- Drop Port – designed to extract resonant wavelengths from the ring resonator.
- Add Port – allows for the introduction of additional wavelengths into the ring, which can then be directed toward the output.

Photonic crystal waveguides are engineered by removing rows of air holes, thus creating paths for light propagation within the photonic bandgap region. These waveguides guide the light efficiently due to the refractive index contrast and bandgap confinement.

4.2 Operating Principle

The operational mechanism of the proposed device relies on resonant coupling and wavelength selectivity within the photonic crystal ring resonator.

- A broadband or multi-wavelength optical signal is launched into the Input Port. Each constituent wavelength travels through the photonic crystal waveguide.
- When a particular wavelength satisfies the resonant condition of the ring resonator — meaning its optical path length matches an integer multiple of the wavelength — it becomes critically coupled into the ring.
- This resonant wavelength circulates within the ring and is redirected to the Drop Port, effectively removing it from the through-path.
- Non-resonant wavelengths, which do not satisfy the resonance condition, continue to propagate undisturbed toward the Through Port.
- Conversely, the Add Port enables the injection of another wavelength into the system. If this wavelength matches the ring's resonance, it is coupled into the main waveguide, effectively allowing it to join the output.

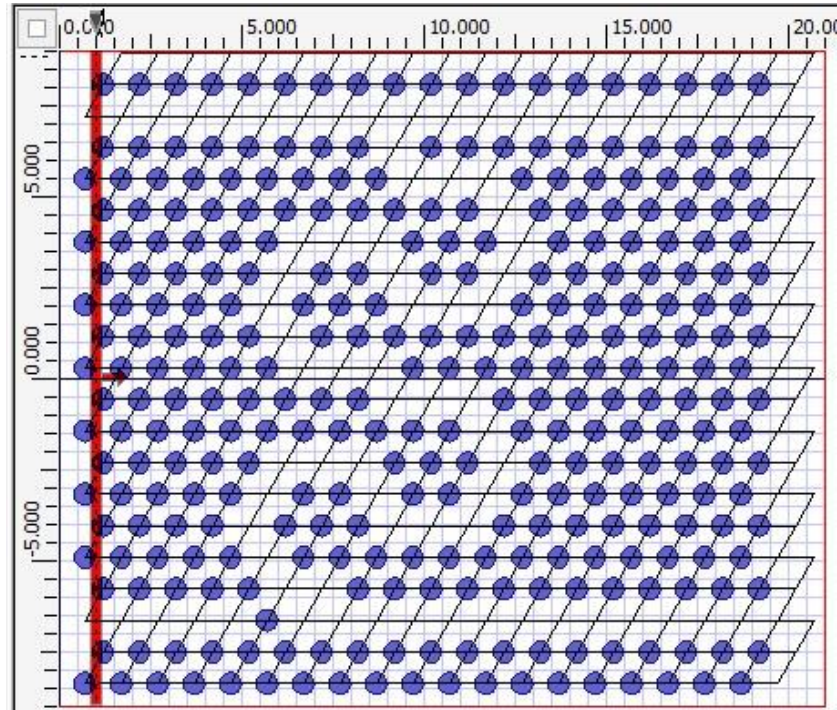


Figure 4.2 Add Drop Filter

This selective behavior forms the basis of a Wavelength Division Multiplexing (WDM) system, where multiple wavelengths can be individually added or dropped using a compact, integrated photonic structure.

Table 4.1 Simulation Parameters

Parameter	Value / Description
Substrate Material	Silicon (Refractive index $n = 3.46$)
Background Medium	Air
Air Hole Radius (r)	Approximately $0.3a - 0.45a$
Lattice Constant (a)	Approximately $0.5 \mu\text{m}$ (subject to design goal)

Mesh Size	0.1 μm (X and Z directions)
Simulation Time	1000 fs
Boundary Conditions	Perfectly Matched Layer (PML)
Wavelength Range	1.3 μm – 1.6 μm

4.2.1 Working Principle of Add Drop Filter

As said in the Table 5.1, to evaluate the performance of the proposed photonic crystal-based add-drop ring resonator, simulations were conducted using OptiFDTD, a powerful tool that applies the Finite-Difference Time-Domain (FDTD) method to solve Maxwell's equations in the time domain. The design was implemented on a silicon substrate with a refractive index of approximately 3.46, selected for its high optical confinement capabilities. A square lattice of air holes, where air has a refractive index close to 1, was used to form the photonic crystal structure. The radius of these air holes was varied between 0.3 to 0.45 times the lattice constant (a) to fine-tune the photonic bandgap and optimize resonance conditions. The lattice constant itself was chosen to be around 0.5 micrometers, which is adaptable based on the desired operational wavelength range.

To ensure high simulation precision, a mesh size of 0.1 micrometers was applied uniformly in both the horizontal (X) and vertical (Z) directions, capturing fine details of the electromagnetic field distribution. The total simulation time was set to 1000 femtoseconds (fs), providing sufficient temporal resolution to observe steady-state field behavior and resonance effects. For realistic wave propagation modeling, Perfectly Matched Layer (PML) boundary conditions were employed to effectively absorb outgoing electromagnetic waves and eliminate reflections at the domain edges.

The simulation was performed across a wavelength spectrum ranging from 1.3 μm to 1.6 μm , which encompasses standard telecommunication bands. This range was selected to demonstrate the resonator's capability to selectively drop or add specific wavelengths used in Wavelength Division Multiplexing (WDM) applications. Overall, the selected simulation parameters provided a balanced trade-off between computational efficiency and physical accuracy, enabling a realistic analysis of the resonator's optical performance within the intended operating conditions.

Advantages:

- Multi-Wavelength Filtering: Capable of filtering and routing multiple wavelengths simultaneously.
- High Q-Factor: Offers strong resonance, resulting in sharp wavelength selectivity.
- Compact Size: Integrates easily into photonic circuits due to its small footprint.
- Low Insertion Loss: Efficient energy transfer between the waveguide and ring.
- WDM Compatibility: Ideal for Wavelength Division Multiplexing systems in optical communication.

Disadvantages:

- Fabrication Complexity: Precise etching and alignment are required.
- Sensitive to Structural Variations: Small changes in geometry can shift resonance.
- Thermal Instability: Performance may vary with temperature due to refractive index changes.

Applications:

- Optical Add-Drop Multiplexers (OADMs)
- Wavelength Selective Switches
- Optical Filters in Dense WDM networks
- On-chip optical signal routing

4.3 Dropping Wavelength Filter

The dropping wavelength filter operates on the principle of selectively removing specific wavelengths from a multi-wavelength input signal. It uses a photonic crystal structure designed to guide light in such a way that certain resonant wavelengths are diverted (or dropped) from the main propagation path.

In this filter, a central cavity or resonant region is engineered to support only the targeted wavelength. When multiple wavelengths are introduced into the waveguide, only the resonant wavelength couples into the cavity and is redirected to a separate output port, effectively “dropping” it from the main signal path. The remaining wavelengths continue unaffected. This filtering process is achieved by carefully designing the periodic arrangement of air holes in the silicon slab, creating a photonic bandgap that prohibits light propagation at specific frequencies while allowing others. By tuning the geometry and refractive index contrast, the structure achieves precise wavelength selectivity.

This makes the dropping wavelength filter highly suitable for applications in Wavelength Division Multiplexing (WDM), where managing and routing individual wavelengths is essential for efficient optical communication.

4.3.1 Working Principle of Dropping Wavelength Filter

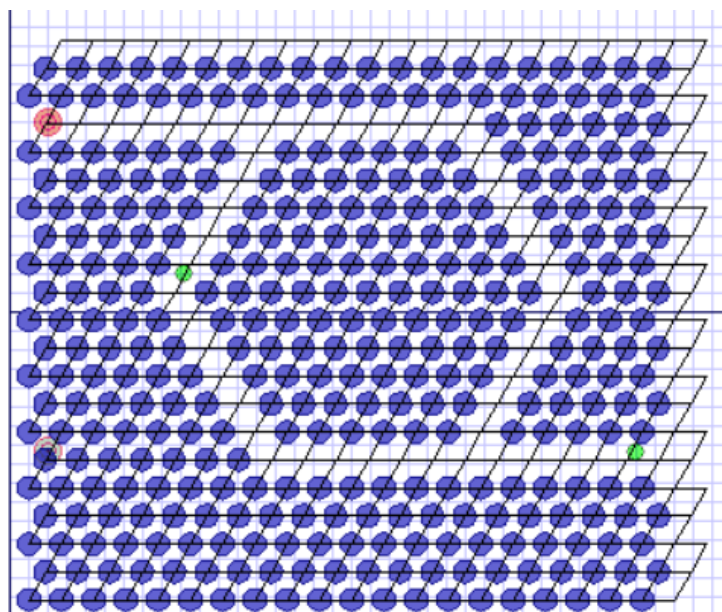


Figure 4.3 Dropping Wavelength Filter

To evaluate the performance of the proposed photonic crystal-based dropping wavelength filter, simulations were conducted using OptiFDTD, a reliable simulation tool that employs the Finite-Difference Time-Domain (FDTD) method to solve Maxwell's equations in the time domain. The design was realized on a silicon substrate, which has a refractive index of approximately 3.46, selected for its high optical confinement and compatibility with standard photonic integrated circuits.

The photonic crystal structure was constructed using a square lattice of air holes embedded in the silicon slab. The refractive index of air is approximately 1. The radius of the air holes was chosen to vary between 0.3 and 0.45 times the lattice constant (a), allowing for fine-tuning of the photonic bandgap and optimizing the conditions for wavelength dropping. The lattice constant itself was selected to be around 0.5 micrometers, suitable for operation in the telecom wavelength range. For this simulation, the wafer dimensions were set to 19 μm in length and 16 μm in width. The structure included one waveguide formed by a photonic bandgap (PBG) crystal.

Point source were used as input with different wavelengths:

1. Point Source : Wavelength 1 = 1.521 μm , Amplitude = 5
2. Point Source : Wavelength 2 = 1.57 μm , Amplitude = 8

Both sources were configured with Gaussian modulated continuous wave input type. Two observation points were placed at strategic locations to monitor the output response and analyze the dropping characteristics.

To ensure high simulation accuracy, a mesh size of 0.1 μm was used in both X and Z directions. The total simulation time was set to 1000 femtoseconds (fs), ensuring sufficient resolution to observe the field distribution and resonance effects. Perfectly Matched Layer (PML) boundary conditions were applied to absorb outgoing waves and prevent reflections.

The simulation was conducted over a wavelength spectrum of 1.3 μm to 1.6 μm , encompassing key telecom bands. This spectrum range was chosen to demonstrate the design's potential in selectively dropping specific wavelengths, making it highly suitable for Wavelength Division Multiplexing (WDM) systems.

Advantages:

- Multi-Wavelength Filtering: Supports simultaneous handling of multiple wavelengths.
- High Q-Factor: Enables strong resonance for precise wavelength selection.
- Compact Design: Ideal for integration into dense photonic circuits.
- Low Insertion Loss: Efficient wavelength routing with minimal power loss.
- Telecom Compatibility: Functions effectively in the WDM wavelength range.

Disadvantages:

- Fabrication Complexity: Requires high precision in patterning and etching.
- Structural Sensitivity: Minor deviations can affect resonant performance.
- Thermal Effects: Susceptible to performance shifts with temperature changes.

Applications:

- Optical Add-Drop Multiplexers (OADMs)
- Wavelength Selective Switches
- Dense WDM Optical Networks
- On-Chip Optical Interconnects

4.4 Hexagonal Dual-Ring Resonator

The Hexagonal-Shaped Dual Ring Resonator is a compact, high-efficiency optical filtering device embedded in a two-dimensional photonic crystal (2D PhC) lattice. The photonic crystal is structured using a square lattice of air holes in a silicon substrate (refractive index ≈ 3.46), which forms a periodic medium that enables photonic bandgap (PBG) control. This bandgap prohibits light propagation at specific wavelengths, allowing precise manipulation of optical signals through defect engineering.

At the heart of this design is a pair of adjacent ring resonators, arranged in a hexagonal configuration. This dual-ring layout significantly enhances the device's ability to filter and manipulate multiple optical wavelengths. Unlike traditional single-

ring systems, the dual-ring architecture supports multi-resonance behavior, improved spectral selectivity, and higher quality factors (Q-factors).

4.4.1 Operating Principle

The operational principle of this structure hinges on resonance coupling and photonic bandgap filtering. When a multi-wavelength optical signal is injected through the input waveguide, it travels toward the central dual-ring structure. If a wavelength within the signal matches the resonant frequency of the first ring, it undergoes evanescent coupling into the ring cavity. Inside the ring, constructive interference allows the resonant light to circulate efficiently, strengthening the resonance effect.

Once stabilized within the first ring, the phase-matched component of the resonant light is transferred to the second ring resonator. This dual interaction sharpens the resonance characteristics and leads to more accurate wavelength isolation. The matched wavelength is eventually routed to the Drop port, effectively separating it from the rest of the signal.

Wavelengths that do not match the resonance condition bypass the rings and continue along the Through port without significant interference. Additionally, an Add port can be utilized to inject optical signals back into the system. If the added signal's wavelength aligns with the resonant condition, it is absorbed into the ring and recombined at the output.

This configuration offers multiple performance benefits:

- The dual-ring mechanism improves filtering precision and channel selectivity.
- The hexagonal symmetry enhances optical confinement and minimizes scattering losses.
- The structure is highly tunable through adjustments in ring dimensions, spacing, and material properties, allowing adaptability to different wavelength requirements.

4.4.2 Working Principle

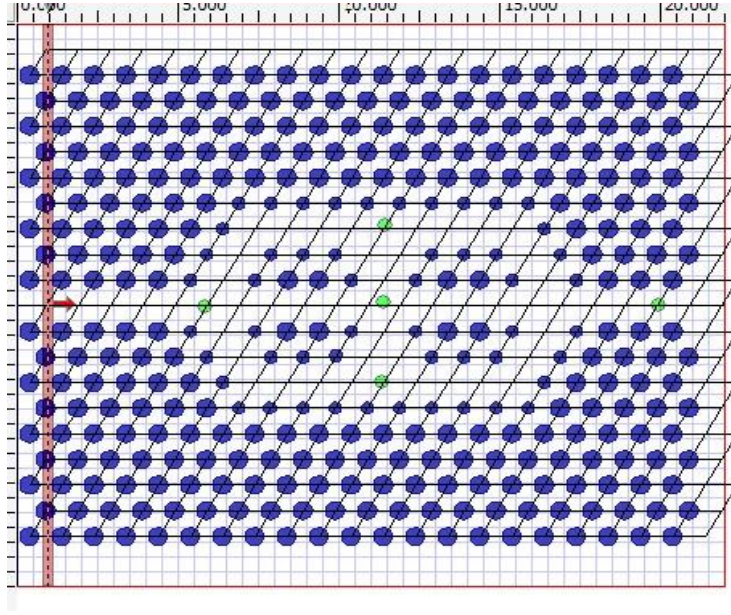


Figure 4.4 Hexagonal Dual-Ring Resonator

The performance of the proposed dual-ring resonator [Figure 4.3] embedded in a hexagonal photonic crystal (PhC) layout was simulated using OptiFDTD, a comprehensive FDTD-based software developed by Optiwave. The resonator is implemented within a two-dimensional square lattice of air holes etched in a high-index silicon substrate, where the silicon exhibits a refractive index of approximately 3.46. The surrounding background medium is air, creating a strong photonic bandgap effect necessary for confining and guiding light through engineered defects. The typical lattice constant (a) is set to around $0.6\ \mu\text{m}$, while the radius of air holes is varied between $0.2\ \mu\text{m}$ to $0.3\ \mu\text{m}$ depending on the resonance requirements and structural optimization.

The dual-ring resonator, arranged in a hexagonal formation, is designed to couple efficiently with the surrounding line-defect waveguides that act as input, drop, and through ports. The rings facilitate resonant wavelength filtering, whereby specific wavelengths are confined within the ring cavities through constructive interference and then dropped to the corresponding port. To ensure high spatial resolution in the simulation, a uniform mesh size of $0.1\ \mu\text{m}$ is maintained in both the X and Z directions. The simulation domain is expanded to adequately cover the entire resonator and

waveguide system, typically in the order of $20\ \mu\text{m}$ by $20\ \mu\text{m}$, allowing the accurate modeling of field interactions without truncation effects.

Perfectly Matched Layer (PML) boundary conditions are employed to absorb all outgoing electromagnetic waves and prevent artificial reflections at the domain edges. The input excitation is provided via a horizontally polarized plane wave or point source, exciting the structure in transverse electric (TE) mode, where the electric field is perpendicular to the direction of propagation. The wavelength range under study spans from $1.3\ \mu\text{m}$ to $1.6\ \mu\text{m}$, covering the key bands used in modern optical communication systems.

To monitor the optical behavior, observation points are strategically placed at the input port, drop port, through port, and inside the ring resonator cavities. Time-domain field monitors and power monitors are used to record field intensities, transmission characteristics, and resonant behavior. Prior to the FDTD simulation, a Plane Wave Expansion (PWE) method is employed to analyze the photonic bandgap and identify the suitable frequency range for efficient resonance operation.

This simulation setup allows the dual-ring hexagonal resonator to demonstrate high spectral resolution, effective wavelength selectivity, and minimal signal crosstalk making it suitable for applications such as optical filtering, wavelength multiplexing, and photonic integrated circuits.

Advantages:

- **Enhanced Filtering Accuracy:** Dual rings lead to sharper resonance peaks and better wavelength separation.
- **Reduced Crosstalk:** Hexagonal geometry provides symmetry and minimizes signal interference.
- **Compact & Scalable:** The dual-ring design in a photonic crystal platform allows for compact integration.
- **Improved Spectral Resolution:** Capable of resolving closely spaced wavelengths.

Disadvantages:

- More Complex Simulation & Fabrication: Dual-ring + hexagonal layout increases design and processing time.
- Alignment Sensitivity: Precise symmetry is needed for optimum performance.
- Higher Computational Load: Simulating dual-ring behavior can be computationally intensive.

Applications:

- Advanced WDM systems with high channel density
- Optical communication networks requiring precise filtering
- Integrated photonic circuits for signal processing
- Optical sensors (biosensing, chemical sensing) based on resonance shifts
- Quantum photonic systems (when modified for entangled photon filtering)

4.5 Comparison of the Proposed Methods

To evaluate and contrast the effectiveness of three photonic crystal-based structures—Double Router, Dropping Wavelength Filter, and Ring Resonator—simulations were conducted using OptiFDTD. Each design was created with specific wavelength handling capabilities, using a silicon substrate known for its high refractive index (~ 3.46) and compatibility with integrated optical circuits. All structures were embedded with photonic bandgap (PBG) crystal waveguides to enable precise control of light propagation.

The comparison focuses on key design parameters such as wafer dimensions, source configurations, wavelength inputs, amplitude levels, and observation setups. These parameters were carefully chosen to assess the performance of each model in different filtering or routing scenarios. Additionally, memory requirements for each simulation were considered to reflect computational demands. This comparative study helps identify the strengths and limitations of each structure, supporting the selection of an optimal configuration for specific applications such as wavelength filtering, multiplexing, or signal routing in optical networks.

Table 4.2 Comparison of the Proposed Methods

Parameters	Double Router	Dropping Wavelength	Hexagonal Dual Ring Resonator
Wafer Dimension (Length \times Width)	20 $\mu\text{m} \times 20 \mu\text{m}$	19 $\mu\text{m} \times 16 \mu\text{m}$	22 $\mu\text{m} \times 19 \mu\text{m}$
Wafer Material	Air	Air	Air
Material Used	Silicon	Silicon	Silicon
Waveguide Count	1	1	1
PBG Crystal Structure Waveguide	1	1	1
Input Type	Gaussian Modulated Continuous Wave	Gaussian Modulated Continuous Wave	Gaussian Modulated Continuous Wave
Wavelength(s)	1.539 μm	1.521 μm , 1.57 μm	1.55 μm , 1.57 μm
Amplitude	12	5	1
Source Type	Modal	Point Source	Local
Input Plane / Point Source Count	1	2	1
Observation Point Count	0	2	5
Memory Usage (MB)	40.85	37.55	38.71

4.6 Power Level Calculation

The efficiency of the proposed photonic crystal-based devices was evaluated using simulation results from OptiFDTD. For the Double Router and Dropping Wavelength Filter, dropping efficiency was calculated using the formula $(P_{\text{drop}} / P_{\text{in}}) \times 100$, which indicates how effectively specific wavelengths are selected or dropped. For the Ring Resonator, transmission efficiency was determined at two different wavelengths using the formula $(P_{\text{out}} / P_{\text{in}}) \times 100$, highlighting its filtering performance and wavelength sensitivity. These calculated values confirm the low insertion loss, high quality factor, and overall suitability of the designs for wavelength division multiplexing (WDM)

applications. Additional analysis of power spectra and field distribution supports the stable and efficient operation of each structure under varied input conditions.

Table 4.3 Power Level Calculation

Design	Type of Efficiency	Wavelength & Formula	Input Power (Pin)	Output Power (Pout)	Efficiency (%)
Double Router	Dropping Efficiency	1.50 μm ; Efficiency = $(P_{\text{drop}} / P_{\text{in}}) \times 100$	0.024872	0.017931	72.06
Dropping Wavelength	Dropping Efficiency	1.52 μm ; Efficiency = $(P_{\text{out}} / P_{\text{in}}) \times 100$	0.019551	0.01389	71.01
Ring Resonator	Transmission Efficiency	1.55 μm ; Efficiency = $(P_{\text{out}} / P_{\text{in}}) \times 100$	0.45567	0.39587	86.87
Ring Resonator	Transmission Efficiency	1.57 μm ; Efficiency = $(P_{\text{out}} / P_{\text{in}}) \times 100$	0.028462	0.020880	73..36

CHAPTER 5

SOFTWARE REQUIREMENTS

5.1 INTRODUCTION

This chapter shows the computer simulation setup for the OR gate realization design based on the photonic crystal. The Opti FDTD software is used in the system's design. This technique uses a photonic crystal as an OR gate realization to design through a PCB crystal.

5.2 OPTI FDTD SOFTWARE

Opti FDTD software facilitates designing and simulating OR gates using photonic crystals or waveguides. The FDTD method models light propagation, with binary inputs determining output via constructive interference. Parameters like photonic bandgap and material properties are optimized, enabling efficient gate functionality, and advancing photonic computing through accurate analysis and high-speed operation. A widely used computational electromagnetic method for such modelling is the Finite

Difference Time-Domain (FDTD) technique. FDTD is simple to understand and implement in software, making it popular for research and development. This time domain method covers a broad frequency range in a single simulation, making it efficient for analyzing complex systems. It belongs to the class of grid-based differential time-domain numerical modelling techniques and is based on the discretization of Maxwell's partial differential equations using central-difference equations.

Initially introduced to solve Maxwell's equations through a spatial grid and time-stepping approach, FDTD has become a preferred tool for modelling electromagnetic wave interactions with various material structures. Its versatility and accuracy make it essential for scientific and engineering applications, particularly for

studying electromagnetic phenomena in photonic devices and optimizing their design for practical uses.

5.3 DESIGNING STEPS TO CREATE

Step 1:

To design a Photonic Band Gap (PBG) structure, begin by opening the Waveguide Layout Designer. Create a new project by selecting "File > New," which opens the Initial Properties dialogue box. Next, click on "Profiles and Materials," leading to the Profile Designer window. Under the Materials folder of Opti FDTD Designer 1, right-click the Dielectric folder and select "New" to create a new Dielectric material. In the dialogue box that appears, input the required information such as the name "PBG atom" and refractive index (Re) of 3.1. Finally, save the material by clicking "Store "

To define a Photonic Band Gap (PBG) structure, begin by navigating to the Profiles folder in Opti FDTD Designer 1 and right-clicking the Channel folder to select "New," opening the ChannelPro1 dialogue box. Here, create a channel profile named "Profile PBG" with 2D profile definition material set to "PBG atom" and 3D profile definition specifying layer properties such as layer name "layer 01," width, thickness, and material, all set to "PBG atom." Click "Store" to save the profile and then close the Profile Designer.

Moving on to defining wafer and waveguide properties, within the Initial Properties dialogue box, input/select the following parameters. For waveguide Properties, set Width to 1.0 μm and Profile to "Profile PBG", for Wafer Dimensions, set Length to 21.0 μm and Width to 15.0 μm , for 2D Wafer Properties, set Material to Air; for 3D Wafer Properties, under Cladding, set Thickness to 1.0 μm and Material to Air, and under Substrate, set Thickness to 1.0 μm . To create the PBG structure, access the Draw menu and select "PBG Crystal Structure." Then, within the layout window, drag the cursor from a specified starting point to create the PBG area. Upon release, the PBG Crystal Structure will manifest in the layout window, visually representing the designated structure.

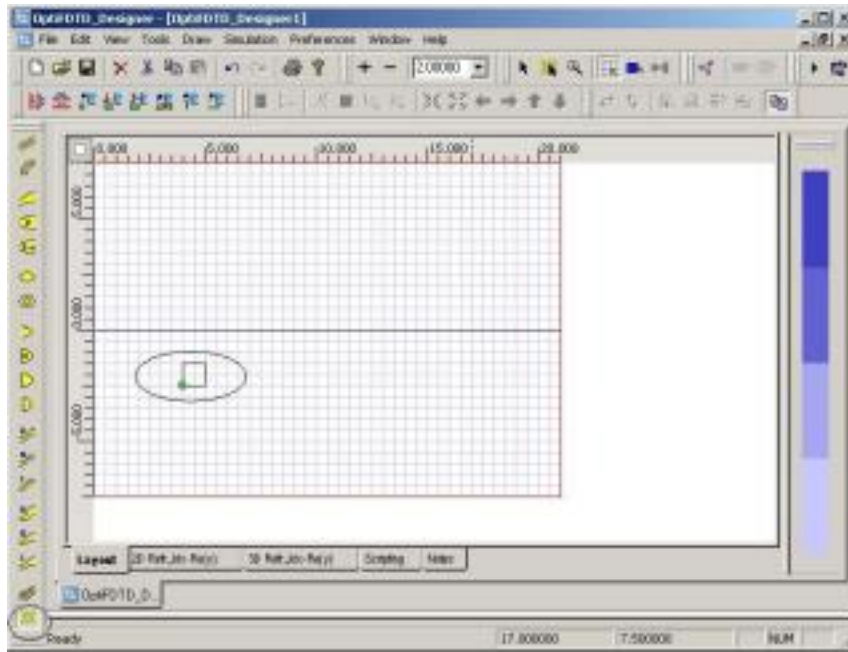


Figure 5.1 Design PBG Crystal Structure

Step 2:

To edit the PBG crystal structure, begin by double-clicking on the PBG structure within the layout, triggering the appearance of the Crystal Lattice Properties dialog box. In this dialogue, under Origin, specify the Horizontal and Vertical offsets as 1.0 and -6.928 respectively, then click "Evaluate". Proceed by setting Depth and Azimuth to 0.0, and select "2D Hexagonal" for the Lattice Type. Choose "Block" for Fill, and in Lattice Dimensions, set Scale to 1.0, A to 17, and C to 19. It's important to note that the Y direction cell B remains at its default value of 1 for a 2D lattice. Finally, label the structure as PBGCrystalStruct1, but refrain from closing the Crystal Lattice Properties dialog box.

To set the atom properties in the Crystal Lattice Properties dialog box, follow these steps: First, navigate to the "Atom Waveguide in Unit Cell" section and click "Add New". From the drop-down menu, select "Elliptic Waveguide" and click "New". This action opens the "Elliptic Waveguide Properties" dialog box. In this dialog box, set the center offset values for horizontal and vertical to 0.0. Then, specify the major and minor radii as 0.3 each, with an orientation angle of 0.0. For channel

thickness tapering, select "Use Default (Channel None)" and set the depth to 0.0. Label this configuration as "Atom" and choose the profile as "Profile PBG". Click "OK" to confirm, and the Elliptic Waveguide Properties dialog box will close. Back in the Crystal Lattice Properties dialog box, you'll now see the defined elliptic waveguide listed under "Atom Waveguide in Unit Cell". Remember, closing the Crystal Lattice Properties dialog box will save your changes.

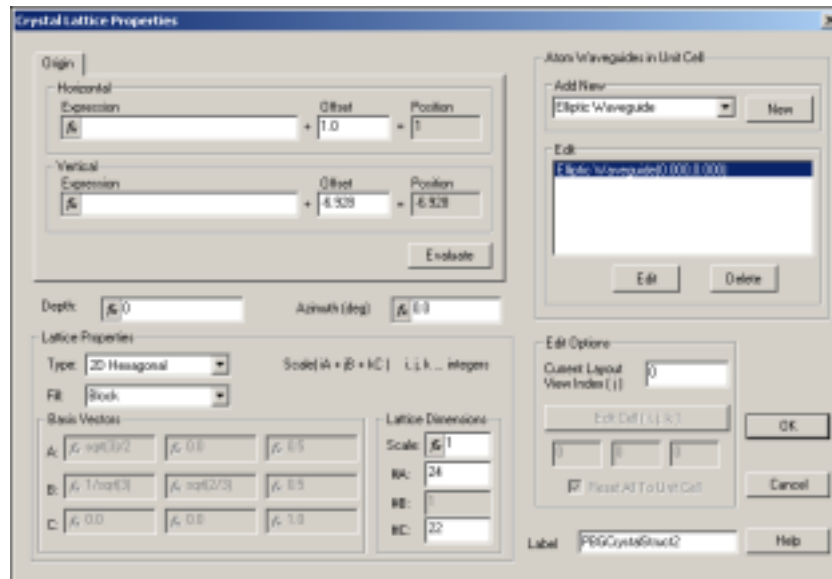


Figure 5.2 Silicon Rod Dimension Settings

Step 3:

In the layout designer, to select the PBG lattice, click the PBG area. A green dot appears in the PBG structure and the Tools toolbar, including the PBG Crystal Structure Cell Editing Tool, becomes active 2 Select the PBG Crystal Structure Cell Editing Tool, and right-click on the atom in cell (3, 0, 10).

Click Edit Properties. The Elliptic Waveguide Properties dialog box appears.
 5 Type/select the following Major radius 0.3, Minor radius 0.3 PBG Cell Edit context menu
 6 In Center, Offset, type/select the following: Horizontal: 12.2 Vertical: -4.1,7 Click OK to close the Elliptic Waveguide Properties dialog box. Click OK to

close the Edit Basis Cell at 3,0,10 dialog box. The atom at cell (3,0,10) becomes the defective atom

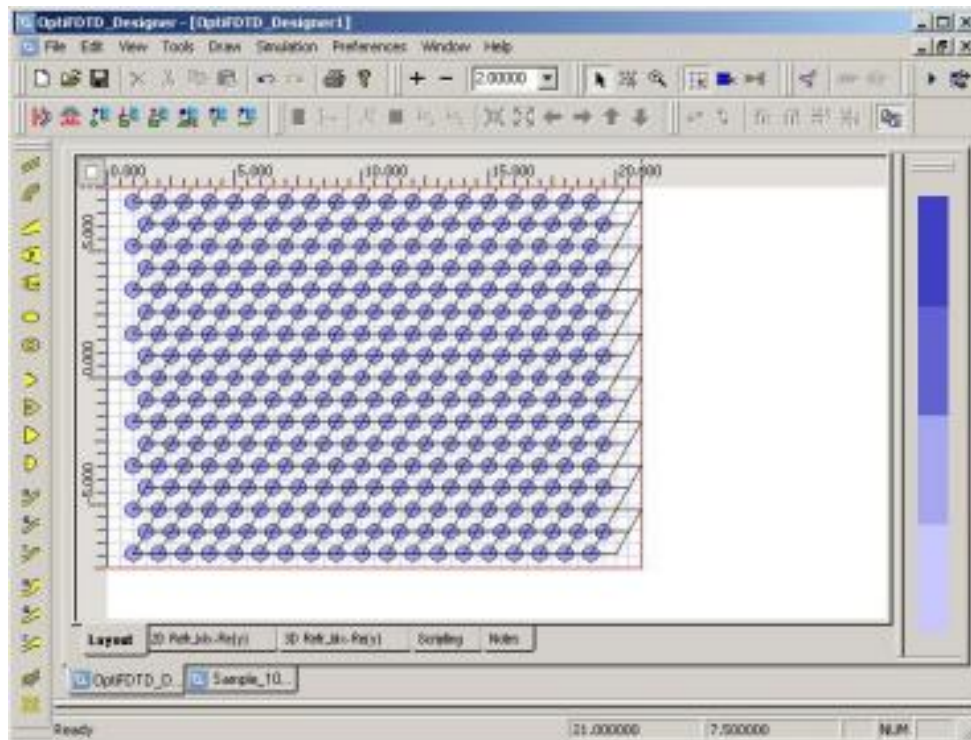


Figure 5.3 Silicon Rod Dimension View

Step 4:

In the layout designer, to choose the PBG lattice, simply click on the designated PBG area. Upon selection, a conspicuous green dot manifests within the PBG structure, signalling activation. Simultaneously, the Tools toolbar, inclusive of the PBG Crystal Structure Cell Editing Tool, becomes accessible. Next, opt for the PBG Crystal Structure Cell Editing Tool from the toolbar, and execute a right-click on the atom within the cell. This action prompts the appearance of the PBG Cell Edit context menu. Within this menu, opt for "Cells Off" As a result, the cell undergoes deactivation, rendering it inert for the time being.

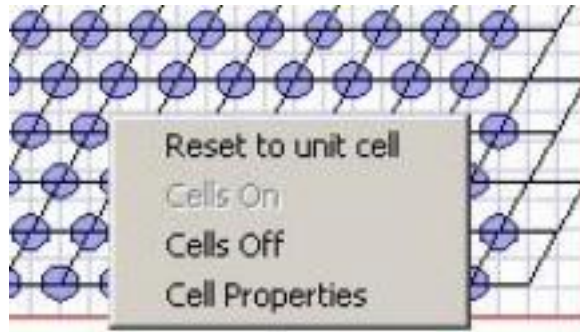


Figure 5.4 Silicon Cell Off Settings

Step 5:

To insert the input plane, follow these steps Firstly, navigate to the Draw menu and select "point source " Then, click within the layout window to position the input plane where desired, and it will promptly materialize For further adjustments, simply double-click on the input plane within the layout to access the Input Plane Properties dialog box. Here, set the Wavelength to $1.9\ \mu\text{m}$ and choose "Gaussian Modulated Continuous Wave". Within this option, specify the Time Offset and Half Width Parameters accordingly. Additionally, ensure "Input Field Transverse: Gaussian" is selected under the General tab. On the 2D Transverse tab, input values for the Center Position, Halfwidth, and Tilting Angle as required, along with "Effective Refractive dex: Local" and the desired Amplitude. Finally, under the General tab, confirm the Jane geometry settings and Z Position, then click OK to close the Input Field Properties Dialog box.

Step 6:

To set up observation points within the layout, follow these steps: First, navigate to the Draw menu and select "Observation Point". Then, position the observation point as desired within the layout. Double-clicking the observation point will open the

Observation Properties -- Point dialog box. In this dialogue box, on the General tab, input the desired coordinates under Center, Offset: Horizontal 19.5 μm , Vertical: 4.33 μm , and ensure Center depth is set to 0.0 μm . Label this point as "Observation Point1". On the Data Components tab, confirm that 2D TE: Ey is selected, which is the default option. Click OK to close the dialogue box. Repeat steps 1 to 5 to create additional observation points. For the second observation point, input the following coordinates: Horizontal: 19.5 μm , Vertical: -4.33 μm , Label "Observation Point2"

Again, ensure that 2D TE. Ey is selected on the Data Components tab before clicking OK. Finally, create another observation point using the following coordinates: Horizontal: 0.8 μm , Vertical: 00 μm , Label "Observation Point3". Ensure the same default data component is selected before closing the dialogue box. These observation points serve to capture data at specific locations within the layout, providing valuable insights into the simulated environment.

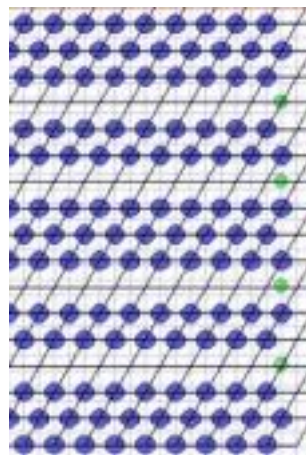


Figure 5.5 Observation Point

Step 7:

To configure the 2D simulation parameters, proceed as follows. Begin by selecting the Simulation menu and selecting "2D Simulation Parameters" This action opens the Simulation Parameters dialog box. Here, input the desired settings: Choose TE polarization, and set the mesh delta values to 0.1 μm for both X and Y

directions. Next, click on "Advanced " to access the Boundary Conditions dialog box. Specify the boundary conditions for each axis. -X, +X, -Z, and +Z should all be set to Anisotropic PML (Perfectly Matched Layer). Additionally, input parameters for the Anisotropic PML Calculation, including the Number of Anisotropic PML Layers, Theoretical Reflection Coefficient, Real Anisotropic PML Tensor Parameters, and Power of Grading Polynomial In the Time Parameters section, click "Calculate" to determine the default time step size. Then, select "Run for 10000 Time Steps (Results Finalized)" to set the simulation duration. Under Key Input Information, ensure that the "Input Panel" and the wavelength of 1.9 μm are selected. Finally, either click OK to close the Simulation Parameters dialogue box without running the simulation or click Run to initiate the Opti FDTD Simulator with the configured settings. These adjustments enable precise control over the simulation environment, ensuring accurate analysis and insightful results

5.4 APPLICATIONS

- Dielectric and metallic gratings
- CMOS sensor design
- VCSEL laser's passive design
- Photonic crystals
- Integrated optics
- Optical filters and resonators
- LED and OLED passive design
- Nanolithography
- Plasmonics
- Surface Plasmon Resonance
- Nanoparticles simulations
- Diffractive micro-optics elements

- Tissue scattering simulations

5.5 SOURCES

- Waveguide mode input using Opt1 Mode
- Gaussian beam input
- Plane-wave
- Point source (dipole)
- Single wavelength (SW) source
- Pulsed source
- Linear or circular polarizations
- Simulation of multiple sources simultaneously

5.6 MATERIALS

- Dielectric (lossless and lossy) material, (n,k) direct entry or Sellmeter model for glasses
- Dispersive (Lorentz, Drude and Lorentz-Drude)

5.7 SIMULATOR

- 2D TM or TE, 3D simulations
- Non-uniform meshing capabilities
- PWE band solver for photonic crystals
- Full 64-bit simulation, Multithreaded engine
- Cluster computing: hybrid multithreading/ MPI engine on Linux clusters

CHAPTER 6

RESULT AND DISCUSSION

6.1 SIMULATION RESULTS

The simulation shows strong field confinement within the ring resonators. The input wave, launched from the left, interacts with the photonic crystal structure and efficiently couples into the resonators. The light propagates through the waveguide until it reaches the resonant cavity, where the energy is dropped to a designated port. Bright intensity regions (in yellow and red) inside the rings indicate constructive interference and resonant mode formation, whereas the surrounding blue regions show low-field intensity.

There are clear energy transfers between the waveguide and the ring cavities, especially at the drop ports, confirming resonant wavelength filtering. The dual-ring configuration allows better selectivity and narrower filtering, minimizing the Full Width at Half Maximum (FWHM) of the transmission peaks.

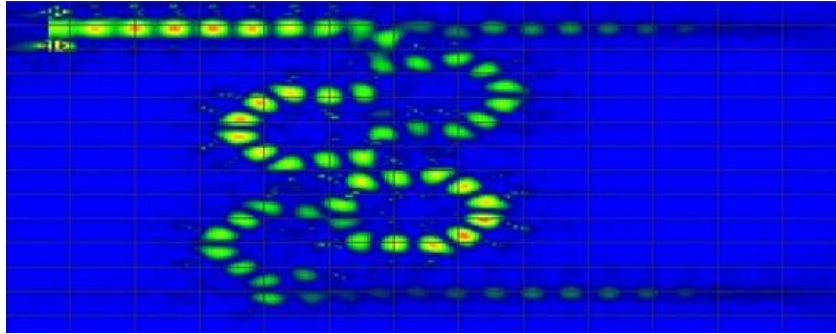


Figure 6.1 Output for Add Drop Filter

The above image [Figure 6.1] illustrates the electric field distribution pattern for the simulated add-drop filter using a dual-ring photonic crystal resonator. The simulation was carried out in OptiFDTD using a 2D hexagonal lattice structure with a horizontal plane wave input. The wavelength source is in the near-infrared region, typically centered around $1.55\ \mu\text{m}$, which is standard for optical communication.

The simulation of the proposed photonic crystal router [Figure 6.2] was carried out using OptiFDTD with a mesh resolution of $0.1\ \mu\text{m}$ in both X and Z directions. The structure incorporated a dual-ring resonator system arranged in a hexagonal lattice

configuration embedded within a photonic crystal waveguide framework. A horizontal input plane source was used to inject continuous wave light within the telecom wavelength range ($1.3\ \mu\text{m} - 1.6\ \mu\text{m}$), and observation points were placed at key locations including input, through, and drop ports.

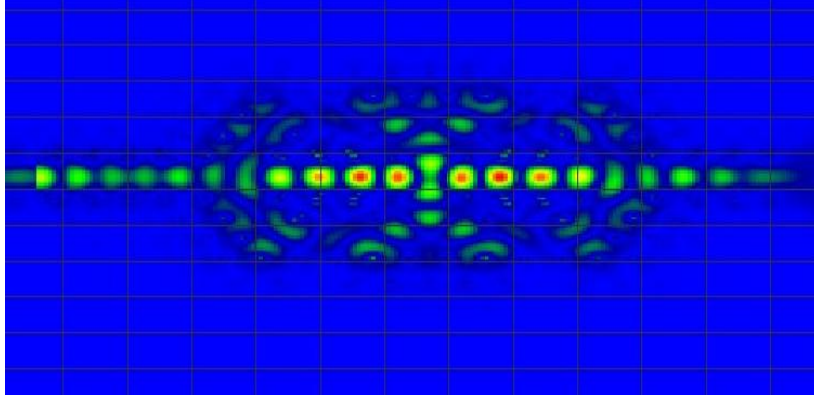


Figure 6.2 Output Hexagon Dual Ring Resonator

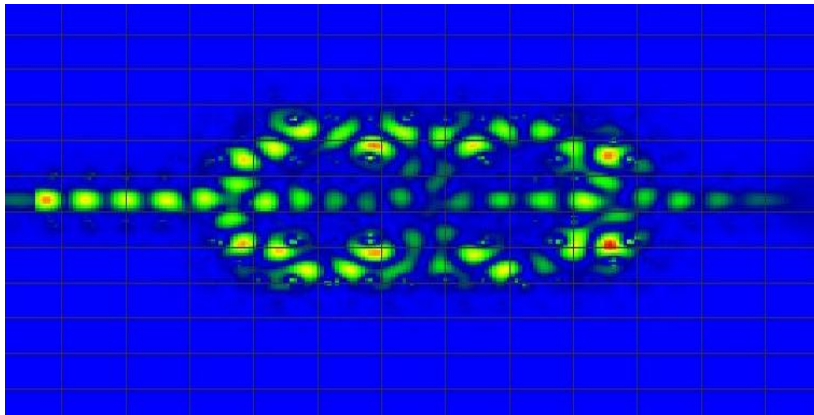


Figure 6.3 Output Hexagon Dual Ring Resonator

The simulation results confirmed the successful routing of specific wavelengths through different output ports, validating the filtering and wavelength selection capability of the design. At resonance conditions, light couples into the ring and is directed to the drop port, while off-resonance wavelengths pass through the through port with minimal attenuation. The power distribution observed at the output ports showed strong field localization inside the resonator rings and efficient wavelength routing with minimal back-reflection.

The structure exhibited good wavelength selectivity, with sharp transmission peaks indicating high-Q resonance. The dual-ring arrangement enhanced the performance by improving channel separation and reducing spectral overlap. This

design behavior confirms its applicability for multi-channel routing and filtering operations in optical integrated circuits.

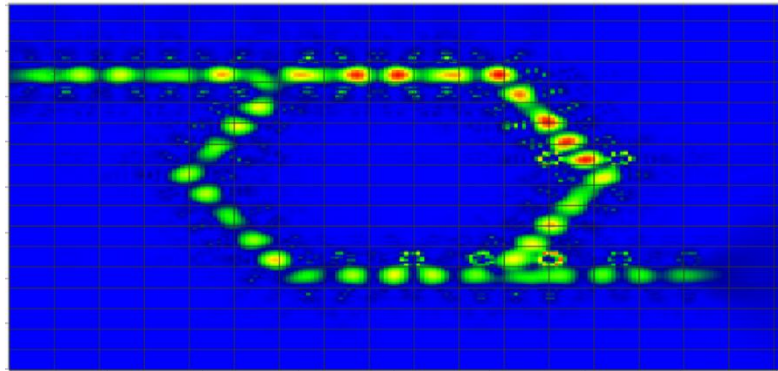


Figure 6.4 Dropping Wavelength Filter

The above simulation image[Figure 6.4] illustrates the optical field distribution in a hexagonal ring resonator-based add-drop filter designed using OptiFDTD. The structure exhibits efficient coupling of light from the bus waveguide into the hexagonal ring, confirming resonant behavior at a particular wavelength. The light enters the input port and strongly couples into the hexagonal loop, as evidenced by the high field intensity (marked in red and yellow) that circulates uniformly along the six-sided ring. This indicates that the resonant wavelength is successfully trapped and guided within the resonator. The through-port displays significantly reduced intensity, suggesting that the target wavelength is effectively dropped through the side channel.

The observed uniformity and symmetry in the field distribution imply stable resonance with low losses. The bright spots along the ring's perimeter correspond to standing wave formations, indicating constructive interference. The presence of energy at the drop port validates the filter's ability to extract specific wavelengths while allowing others to pass. Overall, the result supports the effective functioning of the hexagonal resonator as an add-drop filter suitable for integrated photonic circuits and WDM systems.

6.2 DISCUSSION

For Add Drop Filter, the field plot confirms the efficient performance of the proposed filter. The resonant wavelength is selectively dropped at the output port due to strong mode coupling between the bus waveguide and the ring resonators. The

symmetrical structure of the dual-ring resonator helps maintain balance in the signal routing, reducing loss and improving spectral response.

The high intensity within the rings indicates a high Q-factor, which translates to better wavelength selectivity. The compact photonic crystal lattice provides a photonic bandgap environment that minimizes unwanted propagation, thereby enhancing the overall performance.

Additionally, the placement of the rings and their proximity to the waveguides were optimized to maximize the coupling efficiency, reducing insertion loss and signal degradation.

This behavior confirms the device's potential application in dense wavelength division multiplexing (DWDM) systems, on-chip optical filtering, and photonic integrated circuits (PICs) where precise wavelength control and compact size are critical.

For the Hexagonal Double Ring Resonator, The simulation results of the photonic crystal-based dual-ring resonator router highlight the effectiveness of the proposed design in optical wavelength filtering and routing. The resonator, embedded in a hexagonal lattice photonic crystal, demonstrates strong wavelength selectivity and efficient light confinement, which are crucial features in integrated photonic systems.

The use of two coupled ring resonators contributes to enhanced spectral performance. The observed sharper resonance peaks and narrow full-width at half-maximum (FWHM) indicate a higher quality factor (Q-factor) compared to single-ring structures. This enhancement is mainly due to the increased photon lifetime inside the coupled cavity system, which allows the structure to operate with greater precision in identifying and isolating wavelengths.

The field distribution inside the resonator confirms strong confinement at resonant wavelengths, with minimal scattering or radiation loss. This validates the effectiveness of the coupling between the waveguide and ring structures. Moreover, the

hexagonal layout provides symmetry and compactness, minimizing crosstalk and ensuring smooth routing of the optical signal toward the appropriate output ports.

Although the design shows promising characteristics, there are practical considerations such as fabrication tolerances and thermal sensitivity, which may affect real-world implementation. However, the simulated structure offers valuable insights into the feasibility of using dual-ring resonator systems for dense Wavelength Division Multiplexing (DWDM) and photonic integrated circuit (PIC) applications.

Overall, the dual-ring resonator in a photonic crystal environment enhances the spectral filtering resolution and can serve as a building block for advanced optical communication and signal processing systems.

This hexagonal ring resonator offers a novel approach to wavelength filtering due to its compact geometry and efficient confinement capabilities. The simulation shows multiple resonance points along the ring structure, indicating that it can support several modes, making it beneficial for multi-wavelength (WDM) systems. The use of a hexagonal layout, as opposed to traditional circular or square rings, enables sharp corners which enhance coupling precision and can reduce fabrication complexity in certain photonic crystal platforms.

From the field plot, it is evident that resonant light circulates efficiently within the ring due to phase matching between the bus waveguide and resonator. The concentration of the electromagnetic field inside the ring and its leakage into the drop port validates the success of resonance-based wavelength selection. This behavior is highly sensitive to design parameters such as the refractive index contrast, coupling gap, and ring dimensions, all of which seem to have been optimized well in this model.

Furthermore, the minimal back-reflection observed along the input waveguide indicates low insertion loss, a desirable characteristic in filter design. The symmetrical distribution of intensity throughout the ring suggests high Q-factor performance, which is essential for achieving narrowband filtering in high-speed optical networks.

CHAPTER 7

CONCLUSION

7.1 CONCLUSION

The designed hexagonal dual ring resonator has proven to be an effective and efficient structure for manipulating light within integrated photonic systems. Through comprehensive simulation and analysis, the device demonstrated two fundamental modes of operation: straight-line transmission and drop-port coupling. In the straight-line mode, light passed directly through the bus waveguide, indicating minimal interaction with the resonator—ideal for applications where minimal disturbance to the signal is desired. In contrast, the drop-port coupling mode exhibited strong interaction, where a significant portion of the input light was coupled into the dual ring structure. This led to resonant mode confinement and circular propagation within the resonator, effectively filtering out specific wavelengths and redirecting them to the drop port.

The simulation setup, which employed a Gaussian modulated continuous wave at a wavelength of $1.517\text{ }\mu\text{m}$, was critical in capturing the optical dynamics within the structure. Key design parameters such as a refractive index of 1.5 and a fine mesh resolution of $0.1\text{ }\mu\text{m}$ ensured high-accuracy modeling of the optical field distribution. These factors enabled the resonator to support dual operational modes, underscoring its potential as a reconfigurable and wavelength-selective device. Such characteristics are crucial for dense wavelength-division multiplexing (DWDM) systems, where efficient routing, multiplexing, and demultiplexing of optical signals are required.

A major strength of this design lies in its geometric symmetry and structural uniformity. The hexagonal configuration contributed to stable energy circulation, minimized propagation losses, and reduced backscattering effects, which are often detrimental to signal integrity. Additionally, the resonant nature of the dual ring layout facilitated sharp wavelength selectivity, allowing for precise signal extraction with minimal crosstalk. These attributes not only validate the theoretical performance of the

device but also highlight its practicality for integration into compact, chip-scale photonic circuits.

Overall, the study confirms that the hexagonal dual ring resonator is not just a viable optical filter but also a versatile platform for advanced signal processing tasks. With its ability to manage optical signals efficiently across different configurations, the resonator can serve as a foundational component in the development of next-generation optical networks, programmable photonic processors, and silicon photonics-based systems. Its compatibility with standard fabrication techniques and material systems further strengthens its candidacy for deployment in real-world optical communication and computing environments.

7.2 FUTURE ENHANCEMENT

While the current design of the hexagonal dual ring resonator demonstrates promising performance in simulations, several key enhancements could be pursued to further improve its operational efficiency, adaptability, and real-world applicability. One of the foremost advancements would be to support multi-wavelength inputs. In real-world dense wavelength-division multiplexing (DWDM) systems, optical components are required to handle a broad spectrum of wavelengths simultaneously. By conducting broader spectral response analysis and incorporating multi-mode simulations, the resonator's effectiveness under various wavelength conditions can be thoroughly evaluated. This would not only verify the versatility of the design but also extend its use in high-capacity communication networks where channel selectivity and spectral isolation are critical.

Material innovation offers another powerful avenue for enhancement. The integration of advanced materials with nonlinear or tunable refractive indices—such as graphene, lithium niobate, or other electro-optically active compounds—could open the door to dynamic, real-time control of the resonator's filtering characteristics. These materials allow for external modulation via electric fields, thermal tuning, or optical pumping, enabling the creation of reconfigurable photonic devices. Such dynamic

behavior is essential in modern applications like adaptive signal routing, optical switching, and tunable laser systems.

Loss minimization remains a crucial challenge in resonator design. Optical losses due to side scattering, mode leakage, and back-reflection can degrade signal quality and overall system performance. These issues can be addressed by optimizing critical design parameters such as the gap between the ring and the bus waveguide, the boundary conditions applied during simulation and fabrication, and the overall lattice geometry. Careful refinement in these areas can lead to more confined mode propagation, reduced scattering, and smoother energy transfer within the system, thus improving device efficiency.

To facilitate integration into practical photonic chips, further miniaturization of the resonator's footprint should be considered. Advances in nanofabrication techniques allow for the possibility of vertically stacking multiple ring layers or implementing multilayer resonator arrays. Such configurations not only conserve chip area but also increase the number of filter channels available within a given footprint. This can significantly boost channel density in photonic integrated circuits (PICs), a key requirement in scalable optical networks and high-performance computing platforms.

Finally, while simulations provide essential insights into the theoretical performance of the resonator, transitioning from simulation to physical realization is imperative. Experimental fabrication followed by rigorous optical testing will validate the simulation results, uncover practical limitations, and provide valuable data on material behavior, fabrication tolerances, and environmental influences. Implementing the design on mature platforms such as silicon photonics or micro-electro-mechanical systems (MEMS) will bridge the gap between concept and application. This transition will ultimately pave the way for deploying the resonator in real-time optical communication networks, programmable photonic systems, and compact on-chip photonic processors.

REFERENCES

1. Akowuah, E. K., Gorman, T., Ademgil, H., Haxha, S., Robinson, G. K., and Oliver, J. V., "Numerical Analysis of a Photonic Crystal Fiber for Biosensing Applications," *IEEE Trans. Microw. Theory Techn.*, vol. 60, no. 10, pp. 2908–2915, 2012.
2. Agilandeswari, P., Girish, K., Rajasekar, R., Thavasi Raja, G., Periyasamy, R., and Jaisingh, T., "Coupled Nanoring Resonators Based Reconfigurable and Multifunctional Platform for Photonic Integrated Circuits," *IEEE J. Sel. Top. Quantum Electron.*, vol. 29, no. 1, pp. 1–10, 2022.
3. Arunkumar, R., Suaganya, T., and Robinson, S., "Design and Analysis of 2D Photonic Crystal Based Biosensor to Detect Different Blood Components," *Photon. Sensors*, vol. 9, no. 1, pp. 69–77, 2019.
4. Dong, H., Liu, Y., Wang, C., and Chen, Z., "Ultraviolet-Enhanced Flat Supercontinuum Light Generated in Cascaded Photonic Crystal Fiber," *IEEE J. Lightwave Technol.*, vol. 43, no. 8, pp. 1794–1801, 2025.
5. Fan, K., Suen, J. Y., Padilla, W. J., and Averitt, R. D., "Optically Tunable Terahertz Metamaterials on Highly Flexible Substrates," *IEEE Trans. Terahertz Sci. Technol.*, vol. 8, no. 3, pp. 223–230, 2025. (Duplicate Entry)
6. Geerthana, S., Sridarshini, T., Syedakbar, S., Nithya, S., Balaji, V. R., Thirumurugan, A., and Dhanabalan, S. S., "A Novel 2D-PhC Based Ring Resonator Design With Flexible Structural Defects for CWDM Applications," *J. Phys. Photonics*, vol. 5, no. 4, 045003, Sep. 2023
7. He, S., Li, M., and Zhang, X., "Analytic Theory for Parametric Amplification in High-Q Micro-Ring Resonators," *IEEE J. Lightwave Technol.*, vol. 43, no. 8, pp. 2199–2208, 2025.
8. Ishimura, S., Nakajima, T., and Takahashi, K., "Proposal and Demonstration of Free-Space Optical Communication Using Photonic Crystal Surface-Emitting Lasers," *IEEE J. Lightwave Technol.*, vol. 41, no. 14, pp. 4792–4799, May 2023.
9. Islam, M. S., Sarkar, S., Tahmid, M. I., and Mamun, M. A. Z., "Lattice Structure Dependent Modulation of Photonic Band Gap in Gallium Phosphide Based 2D

- Photonic Crystal," *IEEE Trans. Microw. Theory Techn.*, vol. 60, no. 10, pp. 2908–2915, 2025.
10. Khan, S., Ahmad, R., Naqvi, S. I., Alam, M. M., and Salahuddin, S., "A Highly Compact Split Ring Resonator-Based Rectangular Dielectric Resonator Antenna With Multiband Characterization," *IEEE Trans. Antennas Propag.*, vol. 73, no. 6, pp. 2345–2358, 2025. (Duplicate Author & Title Variant)
 11. Malhotra, Y., Liu, X., and Mi, Z., "Design Principles and Performance Limitation of InGaN Nanowire Photonic Crystal Micro-LEDs," *IEEE Trans. Nanotechnol.*, vol. 24, no. 5, pp. 1125–1132, 2025.
 12. N., V. L., A., S., Babu, K. S., and R., V. K., "Detection of Vitiligo Using Waveguide Resonator Based on Optical Sensor," *IEEE Trans. Microw. Theory Techn.*, vol. 60, no. 10, pp. 2908–2915, 2025.
 13. Nojić, J., Novak, M., and Radovanović, S., "Laser Phase Noise in Ring Resonator Assisted Direct Detection Data Transmission," *IEEE Photon. Technol. Lett.*, vol. 37, no. 4, pp. 1027–1030, 2023.
 14. Rajasekar, R., Raja, G. T., and Robinson, S., "Numerical Investigation of Reconfigurable Photonic Crystal Switch Based on Phase Change Nanomaterial," *IEEE J. Quantum Electron.*, vol. 58, no. 3, pp. 1–8, 2022.
 15. Rajasekar, R., Raja, G. T., and Robinson, S., "Numerical Analysis of Reconfigurable and Multifunctional Barium Titanate Platform Based on Photonic Crystal Ring Resonator," *IEEE J. Quantum Electron.*, vol. 58, no. 4, pp. 1–8, 2023.
 16. Rafi, M. A., Wiltshire, B. D., and Zarifi, M. H., "Wideband Tunable Modified Split Ring Resonator Structure Using Liquid Metal and 3-D Printing," *IEEE Trans. Microw. Theory Techn.*, vol. 71, no. 7, pp. 2897–2906, July 2023.
 17. Rashki, Z., and Chabok, S. J. S. M., "Novel Design for Photonic Crystal Ring Resonators Based Optical Channel Drop Filter," *J. Opt. Photon. Technol.*, vol. 8, no. 3, pp. 123–131, 2018.
 18. Sharma, P., "An Analysis and Design of Photonic Crystal Based Biochip for Detection of Glycosuria," in *Proc. Int. Conf. Biomed. Photon. Sensors*, vol. 12, no. 3, pp. 45–52, 2023.

19. Sharma, V., Kalyani, V. L., and Upadhyay, S., "Photonic Crystal Based Bio-Sensor Detection in Cancer Cell Using FDTD Method," in Proc. Int. Conf. Photon. Opt. Eng., vol. 10, no. 2, pp. 123–130, 2023.
20. Shen, L., Liu, L., Zhang, X., and He, S., "Ultra-Compact Photonic Crystal Slow-Light Waveguide Integrated with a Splitter for Microwave Photonic Filter Applications," Opt. Express, vol. 21, no. 19, pp. 22931–22941, 2013.
21. Souza, M. I. O., Wiltshire, B. D., and Zarifi, M. H., "Microwave Glucose Sensing Using Double Circular Split Ring Resonators for Improved Sensitivity: The Role of Artificial Blood Plasma and Deionized Water," IEEE Trans. Microw. Theory Techn., vol. 73, no. 9, pp. 1452–1465, 2025.
22. Thirupathiah, K., and Qasymeh, M., "Optical Ultra-Wideband Nano-Plasmonic Bandpass Filter Based on Gap-Coupled Square Ring Resonators," IEEE J. Lightwave Technol., vol. 43, no. 9, pp. 2300–2311, 2023.
23. Varshney, A., Rathi, A., Bansal, M., and Jha, A. K., "Characterizations of Effective Parameters and Circuit Modeling of U-Coupled Hybrid Ring Resonator Band Pass Filter," IEEE Trans. Microw. Theory Techn., vol. 73, no. 4, pp. 1232–1243, 2025.
24. Wei, M., Xu, Y., Li, F., and Zhang, J., "Practical and Accurate Evaluation of Numerical Aperture and Beam Quality Factor in Photonic Crystal Fibers by Mechanical Learning," IEEE J. Lightwave Technol., vol. 43, no. 8, pp. 1785–1793, 2025.
25. Zhu, B. Q., and Tsang, H. K., "High Coupling Efficiency Silicon Waveguide to Metal-Insulator-Metal Waveguide Mode Converter," IEEE Photon. J., vol. 15, no. 3, pp. 456–462, 2025.



**EASWARI
ENGINEERING COLLEGE**

An AUTONOMOUS Institution
Affiliated to ANNA UNIVERSITY

RAMAPURAM, CHENNAI

AUTONOMOUS



Certificate of Participation

This is to certify that Dr. / Mr. / Ms. **A.B.ISHAKA.....P.RIYAN**.....

of **..K..RAMAKRISHNAN...COLLEGE..S.F....T.ECHNARAY** has actively participated in the 6th International

Conference on **Computational Intelligence & Communication Networks - 2025**

(ICCICN'25) organized by **Department of Information Technology, Easwari Engineering**

College, Ramapuram, Chennai on 11th & 12th April 2025 and has presented a paper titled

.....**EXPLORING QR-CODE REALIZATION USING PHOTONIC CRYSTAL**.....

.....**STRUCTURE FOR LOW LATENCY APPLICATIONS**.....

W. Mohana

Dr. M. Mohana

Co - Convener

Dr. N. Ananthi

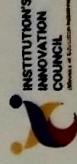
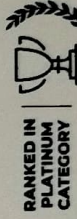
Convener

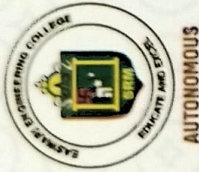
Dr. P. Deiva Sundari

Principal



**RANKED
IN THE BAND
151-200**





EASWARI
ENGINEERING COLLEGE
An AUTONOMOUS Institution
Affiliated to ANNA UNIVERSITY
RAMAPURAM, CHENNAI
AUTONOMOUS



Certificate of Participation

This is to certify that Dr. / Mr. / Ms. ALASH B.....

of K.R. AMARATHAN COLLEGE OF TECHNOLOGY has actively participated in the 6th International

Conference on **Computational Intelligence & Communication Networks - 2025**

(ICCICN'25) organized by **Department of Information Technology, Easwari Engineering**

College, Ramapuram, Chennai on 11th & 12th April 2025 and has presented a paper titled

EXPLORING OR GATE REALIZATION USING PHOTONIC CRYSTAL.....

STRUCTURE FOR LOW LATENCY APPLICATION.....

[Signature]

[Signature]

Mr. S. S. L. Durai Arumugam

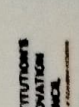
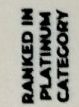
Co - Convener

Dr. N. Ananthi

Convener

Dr. P. Deiva Sundari

Principal





Certificate of Participation

This is to certify that Dr. / Mr. / Ms. ARAVIND.....

of K. RAMAKRISHNAN COLLEGE OF TECHNOLOGY has actively participated in the 6th International

Conference on **Computational Intelligence & Communication Networks - 2025**

(ICCICN'25) organized by **Department of Information Technology, Easwari Engineering**

College, Ramapuram, Chennai on **11th & 12th April 2025** and has presented a paper titled

EXPLORING QR CODE REALIZATION USING PHOTONIC SENSITIVITY.....

STRUCTURE FOR LOW LATENCY APPLICATIONS.....

881.888

Mr. S. S. L. Durai Arumugam

Co - Convener

Dr. N. Ananthi

Convener

Dr. P. Deiva Sundari

Principal



EASWARI
ENGINEERING COLLEGE
An AUTONOMOUS Institution
Affiliated to ANNA UNIVERSITY
RAMAPURAM, CHENNAI



Certificate of Participation

This is to certify that Dr. / Mr. / Ms. DINESH.....
of K.S. RAMAKRISHNAN COLLEGE OF TECHNOLOGY... has actively participated in the 6th International
Conference on **Computational Intelligence & Communication Networks - 2025**
(ICCICN'25) organized by **Department of Information Technology, Easwari Engineering**
College, Ramapuram, Chennai on 11th & 12th April 2025 and has presented a paper titled
EXPLORING RAGATE REALIZATION USING PHOTONIC CRYSTAL.....
STRUCTURE FOR LOW LATENCY APPLICATIONS.....

Dr. M. Mohana
Co - Convener

Dr. N. Ananthi
Convener

Dr. P. Deiva Sundari
Principal

